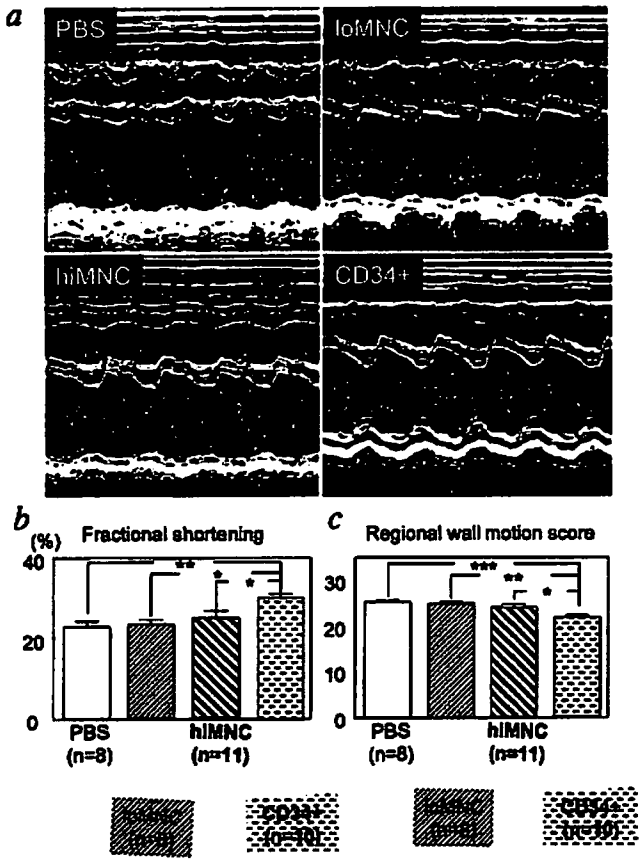

Figure 4. a, Representative M-mode echocardiography 4 weeks after each treatment. b, c, Echocardiographic fractional shortening (b) and regional wall motion score (c) in all treatment groups 4 weeks after MI. *$P<0.05$; **$P<0.01$, ***$P<0.001$.

chemical evidence of abundant human-specific CD45$^+$ cells in rat ischemic myocardium suggests that higher numbers of hematopoietic/inflammatory cells derived from transplanted human cells may play a key role in accelerating myocardial damage after MI in the hiMNC group. Recently, we have reported differentiation of transplanted human CD34$^+$ cells into cardiomyocytes and endothelial cells in infarcted myocardium of nude rats at day 28.[18] The favorable effects of CD34$^+$ cells were proved not only by immunohistochemistry but also by a molecular approach including fluorescent in situ hybridization. In the present study, a similar regenerative property at the chronic phase was immunohistochemically confirmed in the CD34$^+$ cell group but not in the tMNC and PBS groups. The detailed mechanism of the different outcome in each group is unclear; however, loMNCs contain fewer CD34$^+$ cells, which are beneficial for cardiomyogenesis. In the case of hiMNC transplantation, severe hemorrhage/inflammation in the acute phase may be harmful for survival and differentiation of the transplanted cells in the chronic phase. These results indicate that purified CD34$^+$ cell transplantation may have more potential for cardiac myoangiogenesis in the chronic phase of MI compared with total MNC transfer.

Regarding therapeutic potential of the cell therapy after MI, morphometric analyses revealed superiority of CD34$^+$ cell transplantation to tMNC administration. Capillary density in the ischemic myocardium was significantly greater in the hiMNC group than in the PBS and loMNC groups but was superior in the CD34$^+$ cell group compared with the hiMNC group. LV remodeling evaluated by percent fibrosis area also was significantly reduced in the CD34$^+$ cell group compared with all other groups. Percent fibrosis area in the hiMNC group was similar to that in the PBS and loMNC groups despite significant augmentation of ischemic neovascularization. Echocardiographic examinations also demonstrated significantly better outcomes in terms of preservation of both global and regional LV function only in the CD34$^+$ cell group, not in the loMNC and hiMNC groups. These findings suggest that purified CD34$^+$ cells may have more potency for preservation/recovery of LV structural integrity and function in the chronic phase after MI. Taken together with the results in the acute phase after MI, CD34$^+$ cell transplantation may exhibit increased potency and safety in both the acute and chronic phases after MI for therapeutic neovascularization compared with tMNCs. Transplantation of loMNCs may not have significant efficacy for the histological and physiological recovery from MI in the chronic phase despite safety during the acute phase. Moreover, administration of hiMNCs may not achieve a therapeutic effect in the chronic phase equivalent to that of purified CD34$^+$ cells despite equal dosing of CD34$^+$ cells. The diminished effect of hiMNCs in the chronic phase may relate to increased myocardial damage during the acute phase.

A recent clinical report[19] demonstrated that purified CD34$^+$ cells incorporate more efficiently into the ischemic border-zone myocardium after intracoronary infusion compared with unselected tMNCs. In addition to the recent report in the case of intracoronary cell infusion, the present study may provide important information regarding the superiority of CD34$^+$ cells over tMNCs in terms of safety and efficacy after intramyocardial cell transfer.

The present findings provide additional data supporting the selection of specific cell types for applications in myocardial repair after ischemic injury and serve, along with abundant safety data, as the scientific underpinnings for a human pilot clinical trial. These data underscore one of the advantages of cell-based therapies: the ability to actually test the potency of the proposed therapeutic, ie, the human cells themselves. Existing data have documented the varying potency of cells collected from patients with vascular disease and cardiac risk factors.[20] Our findings suggest that within the population of circulating cells, subsets exist that may be safer and more potent for myocardial repair. Further mechanistic data identifying the phenotypic features that define potency will move the field of cell therapy forward.

Acknowledgments

We thank Dr Satoshi Teramukai (Translational Research Informatics, Kobe, Japan) for his statistical advice and Mickey Neely for her secretarial assistance.

Sources of Funding

This study was supported in part by National Institutes of Health grants (HL-53354, HL-57516, HL-63414, HL-77428, HL-80137, and HLP01-66957) and Health and Labor Sciences research grants (H17-trans-002) from the Japanese Ministry of Health, Labor, and Welfare.

Disclosure

Dr Losordo has significant relationships as a principal investigator, collaborator, or consultant on research grants with the following companies: Baxter, Inc, Corautus, Cordis, Curis, Anormed, and Boston Scientific Corp.

References

1. Asahara T, Murohara T, Sullivan A, Silver M, van der Zee R, Li T, Witzenbichler B, Schatteman G, Isner JM. Isolation of putative progenitor endothelial cells for angiogenesis. *Science*. 1997;275:964–967.
2. Kalka C, Masuda H, Takahashi T, Kalka-Moll WM, Silver M, Kearney M, Li T, Isner JM, Asahara T. Transplantation of ex vivo expanded endothelial progenitor cells for therapeutic neovascularization. *Proc Natl Acad Sci U S A*. 2000;97:3422–3427.
3. Murohara T. Therapeutic vasculogenesis using human cord blood-derived endothelial progenitors. *Trends Cardiovasc Med*. 2001;11:303–307.
4. Kawamoto A, Gwon HC, Iwaguro H, Yamaguchi JI, Uchida S, Masuda H, Silver M, Ma H, Kearney M, Isner JM, Asahara T. Therapeutic potential of ex vivo expanded endothelial progenitor cells for myocardial ischemia. *Circulation*. 2001;103:634–637.
5. Kocher AA, Schuster MD, Szabolcs MJ, Takuma S, Burkhoff D, Wang J, Homma S, Edwards NM, Itescu S. Neovascularization of ischemic myocardium by human bone-marrow-derived angioblasts prevents cardiomyocyte apoptosis, reduces remodeling and improves cardiac function. *Nat Med*. 2001;7:430–436.
6. Kawamoto A, Tkebuchava T, Yamaguchi J, Nishimura H, Yoon YS, Milliken C, Uchida S, Masuo O, Iwaguro H, Ma H, Hanley A, Silver M, Kearney M, Losordo DW, Isner JM, Asahara T. Intramyocardial transplantation of autologous endothelial progenitor cells for therapeutic neovascularization of myocardial ischemia. *Circulation*. 2003;107:461–468.
7. Assmus B, Schachinger V, Teupe C, Britten M, Lehmann R, Dobert N, Grunwald F, Aicher A, Urbich C, Martin H, Hoelzer D, Dimmeler S, Zeiher AM. Transplantation of Progenitor Cells and Regeneration Enhancement in Acute Myocardial Infarction (TOPCARE-AMI). *Circulation*. 2002;106:3009–3017.
8. Stamm C, Westphal B, Kleine HD, Petzsch M, Kittner C, Klinge H, Schumichen C, Nienaber CA, Freund M, Steinhoff G. Autologous bone-marrow stem-cell transplantation for myocardial regeneration. *Lancet*. 2003;361:45–46.
9. Fuchs S, Baffour R, Zhou YF, Shou M, Pierre A, Tio FO, Weissman NJ, Leon MB, Epstein SE, Kornowski R. Transendocardial delivery of autologous bone marrow enhances collateral perfusion and regional function in pigs with chronic experimental myocardial ischemia. *J Am Coll Cardiol*. 2001;37:1726–1732.
10. Kamihata H, Matsubara H, Nishiue T, Fujiyama S, Tsutsumi Y, Ozono R, Masaki H, Mori Y, Iba O, Tateishi E, Kosaki A, Shintani S, Murohara T, Imaizumi T, Iwasaka T. Implantation of bone marrow mononuclear cells into ischemic myocardium enhances collateral perfusion and regional function via side supply of angioblasts, angiogenic ligands, and cytokines. *Circulation*. 2001;104:1046–1052.
11. Tateishi-Yuyama E, Matsubara H, Murohara T, Ikeda U, Shintani S, Masaki H, Amano K, Kishimoto Y, Yoshimoto K, Akashi H, Shimada K, Iwasaka T, Imaizumi T. Therapeutic angiogenesis for patients with limb ischaemia by autologous transplantation of bone-marrow cells: a pilot study and a randomised controlled trial. *Lancet*. 2002;360:427–435.
12. Perin EC, Dohmann HF, Borojevic R, Silva SA, Sousa AL, Mesquita CT, Rossi MI, Carvalho AC, Dutra HS, Dohmann HJ, Silva GV, Belem L, Vivacqua R, Rangel FO, Esporcatte R, Geng YJ, Vaughn WK, Assad JA, Mesquita ET, Willerson JT. Transendocardial, autologous bone marrow cell transplantation for severe, chronic ischemic heart failure. *Circulation*. 2003;107:2294–2302.
13. Schiller NB, Shah PM, Crawford M, DeMaria A, Devereux R, Feigenbaum H, Gutgesell H, Reichek N, Sahn D, Schnittger I. Recommendations for quantitation of the left ventricle by two-dimensional echocardiography: American Society of Echocardiography Committee on Standards, Subcommittee on Quantitation of Two-Dimensional Echocardiograms. *J Am Soc Echocardiogr*. 1989;2:358–367.
14. Grigg AP, Roberts AW, Raunow H, Houghton S, Layton JE, Boyd AW, McGrath KM, Maher D. Optimizing dose and scheduling of filgrastim (granulocyte colony-stimulating factor) for mobilization and collection of peripheral blood progenitor cells in normal volunteers. *Blood*. 1995;86:4437–4445.
15. Martinez C, Urbano-Ispizua A, Rozman C, Marin P, Mazzara R, Carreras E, Rovira M, Sierra J, Briones J, Ordinas A, Montserrat E. Effects of G-CSF administration and peripheral blood progenitor cell collection in 20 healthy donors. *Ann Hematol*. 1996;72:269–272.
16. Pislaru SV, Barrios L, Stassen T, Jun L, Pislaru C, Van de Werf F. Infarct size, myocardial hemorrhage, and recovery of function after mechanical versus pharmacological reperfusion: effects of lytic state and occlusion time. *Circulation*. 1997;96:659–666.
17. Asanuma T, Tanabe K, Ochiai K, Yoshitomi H, Nakamura K, Murakami Y, Sano K, Shimada T, Murakami R, Morioka S, Beppu S. Relationship between progressive microvascular damage and intramyocardial hemorrhage in patients with reperfused anterior myocardial infarction: myocardial contrast echocardiographic study. *Circulation*. 1997;96:448–453.
18. Iwasaki H, Kawamoto A, Ishikawa M, Oyamada A, Nakamori S, Nishimura H, Sadamoto K, Horii M, Matsumoto T, Murasawa S, Shibata T, Suehiro S, Asahara T. Dose-dependent contribution of CD34-positive cell transplantation to concurrent vasculogenesis and cardiomyogenesis for functional regenerative recovery after myocardial infarction. *Circulation*. 2006;113:1311–1325.
19. Hofmann M, Wollert KC, Meyer GP, Menke A, Arseniev L, Hertenstein B, Ganser A, Knapp WH, Drexler H. Monitoring of bone marrow cell homing into the infarcted human myocardium. *Circulation*. 2005;111:2198–2202.
20. Vasa M, Fichtlscherer S, Aicher A, Adler K, Urbich C, Martin H, Zeiher AM, Dimmeler S. Number and migratory activity of circulating endothelial progenitor cells inversely correlate with risk factors for coronary artery disease. *Circ Res*. 2001;89:E1–E7.

CLINICAL PERSPECTIVE

These preclinical studies provide evidence for increased safety and potency of CD34+ cell therapy for treatment of myocardial ischemia and form the basis for a recently completed phase 1/2 clinical trial. The selection of CD34+ cells was originally performed in the setting of stem cell transplantation for reconstitution of hematopoiesis; however, it became apparent that in many settings the unselected mononuclear cell population also was capable of achieving this goal, and the selection procedure was largely abandoned in that context. The present studies were designed to determine whether this was also the case when the CD34+ stem cell was used for neovascularization of ischemic tissue. The data reveal that all parameters of safety and efficacy are significantly improved after intramyocardial transplantation of CD34+ cells compared with treatment with an equal dose (cell number) of unselected mononuclear cells. The same was true when the mononuclear cell dose was adjusted to achieve an equivalent dose of CD34+ cells, suggesting that the unselected cells contain elements that impair the salutary effects of CD34+ cells on myocardial repair. These data provide further evidence that the CD34+ cell is a suitable platform for cell-based ischemic tissue repair and that selected cells offer a safety and potency advantage.

Synchrotron Radiation Coronary Microangiography for Morphometric and Physiological Evaluation of Myocardial Neovascularization Induced by Endothelial Progenitor Cell Transplantation

Hiroto Iwasaki, Kazuhito Fukushima, Atsuhiko Kawamoto, Keiji Umetani, Akira Oyamada, Saeko Hayashi, Tomoyuki Matsumoto, Masakazu Ishikawa, Toshihiko Shibata, Hiromi Nishimura, Hidekazu Hirai, Yutaka Mifune, Miki Horii, Kazuro Sugimura, Shigefumi Suehiro, Takayuki Asahara

Background—Therapeutic effect of stem cell transplantation (SCTx) for myocardial neovascularization has been evaluated by histological capillary density in small animals. However, it has been technically difficult to obtain imaging evidence of collateral formation by conventional angiography.

Methods and Results—Peripheral blood CD34+ and CD34− cells were isolated from patients with critical limb ischemia. PBS, CD34− cells, or CD34+ cells were intramyocardially transplanted after ligating LAD of nude rats. Coronary angiography of ex vivo beating hearts 5 and 28 days after the treatment was performed using the third generation synchrotron radiation microangiography (SRM), which has potential to visualize vessels as small as 20 μm in diameter. The SRM was performed pre and post sodium nitroprusside (SNP) to examine vascular physiology at each time point. Diameter of most collateral vessels was 20 to 120 μm, apparently invisible size in conventional angiography. Rentrop scores at day 28 pre and post SNP were significantly greater in CD34+ cell group than other groups ($P<0.01$). To quantify the extent of collateral formation, angiographic microvessel density (AMVD) in the occluded LAD area was analyzed. AMVD on day 28 post SNP, not pre SNP, was significantly augmented in CD34+ cell group than other groups ($P<0.05$). AMVD post SNP closely correlated with histological capillary density ($R=0.82$, $P<0.0001$).

Conclusions—The SRM, capable of visualizing microvessels, may be useful for morphometric and physiological evaluation of coronary collateral formation by SCTx. The novel imaging system may be an essential tool in future preclinical/translational research of stem cell biology. (***Arterioscler Thromb Vasc Biol.*** **2007;27:1326-1333.**)

Key Words: synchrotron radiation microangiography ■ image ■ CD34+ cells ■ neovascularization ■ myocardial infarction

Stem/progenitor cell transplantation (SCTx) investigated since the early 1990s is a novel approach for vascular regeneration therapy in ischemic diseases.[1-3] One of the examples of the SCTx is transplantation of adult peripheral blood CD34+ cells that are endothelial progenitor cell (EPC)-enriched population. Transplantation of CD34+ cells prevents left ventricular (LV) dilatation and wall thinning, inhibits myocardial fibrosis and apoptosis, and preserves LV function through augmentation of myocardial neovascularization and blood flow.[4-9] Evidence of increased vascularity by therapeutic neovascularization such as CD34+ cell transplantation has been obtained by histological assessment of capillary density and physiological evaluation of tissue perfusion has been by microsphere methods in small sized animals (mice and rats) with acute MI.[10] However, the histological examination has limitation for precise assessment of vascular physiology in response to environmental stress. Though microsphere assessment was performed to evaluate physiological blood flow, it was pointed out to lack significant reproducibility in small animal models. Several research groups have utilized other approaches such as corrosion casts[11,12] and angiography[13,14] to visualize collateral vessels.

Original received November 29, 2006; final version accepted February 12, 2007.

From Stem Cell Translational Research (H.I., A.K., A.O., S.H., T.M., M.I., H.N., Y.M., M.H., T.A.), Kobe Institute of Biomedical Research and Innovation/RIKEN Center for Developmental Biology; the Department of Cardiovascular Surgery (H.I., T.S., H.H., S.S.), Osaka City University Graduate School of Medicine; the Department of Image-based Medicine (K.F.), Kobe Institute of Biomedical Research and Innovation; the Department of Radiology (K.F., K.S.), Kobe University Graduate School of Medicine; the Research & Utilization Division (K.U.), Japan Synchrotron Radiation Research Institute, SPring-8, Sayo; and the Department of Regenerative Medicine Science (T.A.), Tokai University School of Medicine, Isehara, Japan.

H.I. and K.F. contributed equally to this work.

Correspondence to Takayuki Asahara, MD, Stem Cell Translational Research, Kobe Institute of Biomedical Research and Innovation/RIKEN Center for Developmental Biology, 2-2 Minatojima-Minamimachi, Chuo-ku, Kobe 650-0047, Japan. E-mail asa777@aol.com

Arterioscler Thromb Vasc Biol. is available at http://www.atvbaha.org DOI: 10.1161/ATVBAHA.106.137141

Corrosion casts allow the visualization of small arteries less than 100 μm in diameter,[11] although it is impossible to examine in live animals or ex vivo beating hearts, and the complete distension of the vessels depends on several factors such as elastic properties of the vessel wall, viscosity of the infused material, and pressure of infusion. Conventional angiography, which has been widely performed in clinical practice, can be also undergone in live animals repeatedly. However, previous reports indicated that conventional angiography systems, which could not visualize arteries less than 200 μm in diameter,[15,16] have insufficient resolution to visualize full extent of collateral formation. The resolutional limitation may lead to underestimation of angiogenic potential of the SCTx, because improvement of collateral-dependent flow typically results from the proliferation of vessels less than 180 μm in diameter.[17–19] The indispensable angiographic assessment in small animals has never been established.

Synchrotron radiation (SR) has been investigated as a novel approach for animal studies because intravenous coronary angiography, a relatively less invasive technique compared with selective coronary angiography, was begun at the end of 1970's. Research groups have improved imaging systems in SR facilities for future clinical application.[20] Aside from the intravenous coronary angiography, Mori et al[15,16] recently developed a new angiography system called SR microangiography (SRM), which was an intraarterial microangiography system. In this system, monochromatic SR is used as an x-ray source, which energy was adjusted to 33.2 keV just above the iodine K-edge energy to produce the highest contrast image of the iodine contrast material, and a high-fidelity video system is also used as a detector, which has the potential to visualize small vessels (diameter <50 to 100 μm). Thereafter, many researchers have used the SRM to visualize penetrating transmural coronary arteries in the canine hearts,[21] collateral microvessels following therapeutic angiogenesis in rat model of hind limb ischemia,[22] vasodilatation of arterial circle of cerebrum and its branches of the dogs,[23] and tumor-derived angiogenic vessels of the rabbits[24] at the Photon Factory in Tsukuba, Japan. However, the previous SRM system was unable to visualize coronary arteries, their branches, and collateral vessels in beating hearts of small animals because of the still inappropriate image quality. Currently, new SRM system with spatial resolution in the μm range has been developed in the SPring-8 (Japan Synchrotron Radiation Research Institute) in Sayo, Japan. Recently, Kidoguchi et al[25] have applied the new SRM system to visualize branches of rat middle cerebral arteries and successfully depict the vessels as small as 30 μm in diameter at 9.5 μm of detector pixel size. In this study, we used the new generation SRM to visualize rat coronary vessels as small as 20 μm in diameter at 4.5 μm of pixel size and evaluated coronary vascular function in response to vasodilator under fast beating condition. Here, we report usefulness of the third generation SRM to visualize collateral vessels and quantify the effect of therapeutic neovascularization by bone marrow (BM)-derived CD34+ cell transplantation in rats with MI.

Methods

Isolation of CD34+ Cells From Patients With Critical Limb Ischemia

Peripheral blood total mononuclear cells (tMNCs) were obtained from 3 male patients 71, 63, and 60 years of age with atherosclerotic peripheral artery disease by apheresis after 5-day subcutaneous administration of G-colony stimulating factor (CSF) (10 μg/kg/d). CD34+ cells or CD34− cells were isolated from the tMNCs by a magnetic cell sorting system, CliniMACS (Miltenyi Biotec).[26] The CD34+ cell fraction had a purity of >99%, as determined by fluorescence-activated cell sorting (FACS) analysis using a monoclonal antibody specific for human CD34 (Becton Dickinson). CD34+ cells in this study were $CD31^{bright}$, $AC133^{bright}$, and $CD45^{dim}$ but negative for KDR and VE-cadherin. In contrast, CD34− cells were positive for CD45 and CD31, but negative for AC133, KDR, and VE-cadherin. The FACS results suggest that freshly-isolated CD34+ cells are immature population responsible for hematopoietic stem cells, endothelial progenitor cells, and hemangioblasts, whereas the CD34− cells are not considered to be either immature or mature endothelial lineage cells (supplemental Figure I, available online at http://atvb.ahajournals.org).

These patients received intramuscular transplantation of 10^5 CD34+ cells/kg according to the protocol of a phase I/II dose-escalation clinical trial. Remaining CD34+ or CD34− cells were used for following experiments. Informed consent regarding the cell therapy and experimental use of the remaining cells was obtained from each patient before the case registration. The clinical study protocol was approved by the Institutional Ethics Committees of Kobe Institute of Biomedical Research and Innovation and Kobe City General Hospital.

Animals

Female athymic nude rats (F344/N Jcl rnu/rnu; CLEA Japan, Tokyo, Japan) aged 7 to 8 weeks and weighing 145–160 g were used in this study. The Institutional Animal Care and Use Committees of RIKEN Center for Developmental Biology approved all animal procedures including human cell transplantation. All of our experiments on imaging of the rat hearts with MI also conformed to the SPring-8 Guide for Care and Use of Laboratory Animals in SRM examination.

Induction of Myocardial Infarction and Cell Transplantation

Rats were anesthetized with ketamine and xylazine (60 mg/kg and 10 mg/kg, respectively, IP). MI was induced by ligating left anterior descending coronary artery (LAD) as described previously.[7–9] Twenty minutes after MI, rats received intramyocardial transplantation of 1×10^5 CD34− cells or 1×10^5 CD34+ cells resuspended with 100 μL of PBS or the same volume of PBS without cells (n=9 in each group). To evaluate incorporation and development of the transplanted cells in MI tissue, CD34+ cells or CD34− cells labeled with fluorescent carbocyamine 1, 1′-dioctadecyl1–1 to 3,3,3,3′-tetramethylindocarbocyanine perchlorate (DiI) dye (Molecular Probes, Carlsbad, CA) were intramyocardially transferred into athmic nude rats (n=3) after MI.[9]

Imaging System

SRM experiments were performed at the 2nd optical hatch of the BL28B2 beamline in the SPring-8. Monochromatic synchrotron radiation with an energy level of 33.2 keV was obtained from the beamline. An X-ray imaging system needs to have high shutter speed to make sharp and blur-free images of fast-moving hearts, and for this purpose we developed a shutter system using a rotating disk with radial slots rotating around an axis parallel to the X-ray beam. The shortest shutter open time was 0.1 ms. X-rays transmitted through the object are detected by the X-ray direct-conversion type detector incorporating the X-ray SATICON pick-up tube. For high-resolution, real-time imaging (7.0 μm or 4.5 μm pixel size, 30 frames/second), the monochromatized x-ray obtained from the third generation SR source and the new rotating disk shatter were used.

Differences in Characteristics of Synchrotron Radiation System Between the Photon Factory and the SPring-8

	Photon Factory	SPring-8
Input field of view, mm	50×50 or 20×20	7.0×7.0 or 4.5×4.5
Pixel size, μm	48×48 or 19×19	7.×7.0 or 4.5×4.5
Spatial resolution, μm	30	6
Minimum detectable vessel diameter, μm	50–100	20
Shortest shutter open time, msec	17	2

Sequential images were obtained with an input field of view of 7.0 mm × 7.0 mm or 4.5 mm × 4.5 mm. Image signals were converted into digital format and stored in a frame memory with a 1024×1024 pixels format and 10-bit resolution. Improved points in the new generation SR imaging system in the Spring-8 compared with the previous version in the Photon Factory in Tsukuba, Japan is shown in the Table.

Coronary Microangiography

Transplanted immunodeficient rats were anesthetized with pentobarbital and anticoagulant heparin intraperitoneally. After thoracotomy, the heart and aortic arch were rapidly excised and immersed in perfusion solution. The pericardium was quickly removed under immersion and aorta was prepared for cannulation. The heart was mounted on an aortic cannula, and then pulmonary artery was cut near its origin. Throughout the experiment, aortic retrograde perfusion at a constant flow rate (4.0 mL/min) with oxygenated perfusion solution drawn from a temperature-regulated reservoir (37°C) was started according to the Langendorf technique, as described in detail previously.[27] The perfusion solution was of the following composition (in mmol/L): NaCl, 118.5; $NaHCO_3$, 25.0; KCl, 3.2; $MgSO_4$, 1.2; KH_2PO_4, 1.2; $CaCl_2$, 1.4; glucose, 11.0. The solution was filtered before use and gassed continuously with 90% O_2/10% CO_2 (pH 7.4 at 37°C). Perfusion fluid was directed into coronary arteries to perfuse the entire ventricular mass of the heart. Contractile function and regular heart rhythm returned within a few seconds, and maximum function was established in several minutes. After stabilization of heart rate and perfusion pressure in the ex vivo beating hearts under the Langendorf perfusion, SRM at baseline was performed in each animal. The microangiographic images were taken at base, mitral papillary muscle, and apical levels. Microangiography was performed with an automated injector (Nemoto Kyorindo) which was programmed to reproducibly deliver 0.4 mL/sec of nonionic contrast media containing 37% iodine (Iopamiron 370; Nihon Schering) for 4 sec. After the baseline angiography were taken, sodium nitroprusside (SNP) (Roche), an endothelium-nondependent vasodilator, was added to oxigenized Krebs-Henseleit solution while keeping the perfusate concentrations and the flow rate. The concentration of SNP used in this study was 1×10^{-6} mol/L, which corresponds to values validated as the most suitable concentration of SNP to assess the vasodilating effect in a previous study.[28] Microangiography was similarly performed to visualize dilated coronary vessels. Each imaging started 1 to 2 seconds before contrast media infusion, so that background pictures without contrast media could be taken for later computed analysis.

Tissue Harvest

After SRM, hearts were sliced in a broad-leaf fashion into 4 transverse sections from apex to base, embedded in OCT compound, snap frozen in liquid nitrogen (LN_2), and stored at −80°C for immunohistochemistry. Rat hearts in OCT blocks were sectioned, and 5-μm serial sections were collected on slides followed by fixation with 4.0% paraformaldehyde at 4°C for 5 minutes and stained immediately. Total RNA was isolated by selective dissection of peri-infarct area in LV myocardium for reverse transcriptase-polymerase chain reaction (RT-PCR).

Angiographic Assessment of Collateral Vessel Formation

Collateral flow filling to the LAD territory pre and post SNP was graded angiographically in a blinded manner by use of the Rentrop scoring system.[7] To quantify development of collateral vessels, angiographic microvessel density (AMVD) in the occluded LAD area both pre and post SNP was measured by following computed analysis. Hearts were divided into 4 parts from ligation point to apex, then we measured vessel densities in each part. Region of interest was determined in LAD perfusing area but without visible major branches of the LAD. The images immediate before (background) and during contrast media infusion were captured by an image scanner. After the image capture, vessel density in each part was obtained by subtracting the background density from the angiographic density processed with the NIH image program (v. 1.62) as described previously.[29] Average value of the vessel densities in 4 portions was calculated as the AMVD for each imaging procedure. The ratio of AMVD post SNP to pre SNP (AMVD ratio) was also calculated. These data analyses were performed by 2 blinded observers.

Morphometric Evaluation of Capillary Density

Histochemical staining with isolectin B4 (Vector Laboratories) was performed, and capillaries were recognized as tubular structures positive for isolectin B4. Histological capillary density was evaluated by morphometric examination of 5 randomly selected fields of tissue sections recovered from segments of LV myocardium subserved by the occluded LAD.[7–9] All morphometric studies were performed by 2 examiners who were blinded to treatment.

Statistical Analysis

The results were statistically analyzed with the use of a software package (Statview 5.0, Abacus Concepts Inc). All values were expressed as mean±SE. Paired *t* tests were performed for comparison of data between day 5 and day 28, and between pre and post SNP infusion. The comparisons among 3 groups were made with 1-way ANOVAs. Post hoc analysis was performed by Fisher protected least significant difference test. Correlation between histological and microangiographic vessel densities was analyzed by linear regression test. Differences of $P<0.05$ were considered statistically significant.

Results

Rentrop Score Pre and Post SNP Infusion

SRM was performed to evaluate collateral vessel development by elucidating Rentrop score, a semiquantitative grading of collateral flow filling into the occluded coronary artery,[10] 5 and 28 days after cell transplantation. SRM on day 5 demonstrated that the LAD was totally occluded at the ligation point and collateral flow filling into the distal LAD was not well visualized in all groups (Figure 1a). Angiographic Rentrop score at day 5 was not significantly different in each group (Figure 1c). In contrast, SRM on day 28 revealed better visualization of collateral vessels into the distal LAD area in CD34+ cell group compared with both CD34− cell and PBS groups. Collateral vessels were generated from left circumflex artery or proximal site of LAD. Diameter of the collateral vessels was generally 20 to 120 μm, which is apparently invisible size in conventional angiography (Figure 2a). Rentrop score at day 28 was significantly greater in CD34+ cell group than either CD34− cell or PBS group (CD34+, 1.6±0.2; CD34−, 0.6±0.2; PBS, 0.4±0.2, $P<0.01$ for CD34+ versus CD34− and PBS) (Figure 2c).

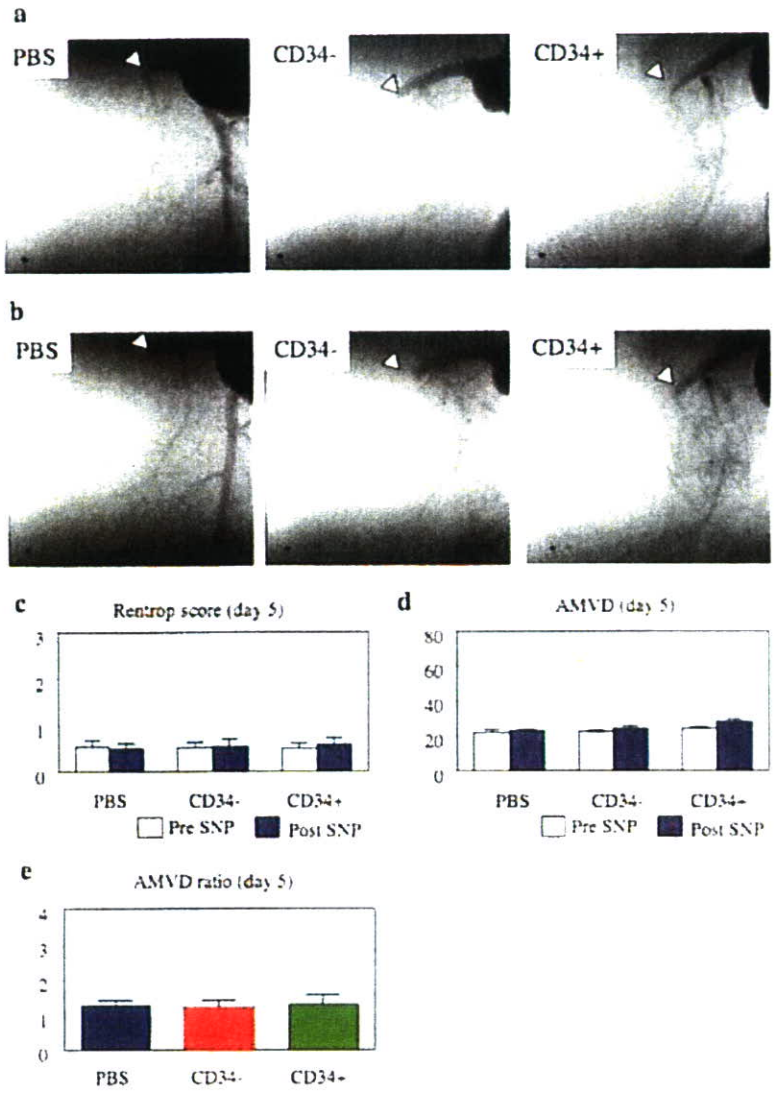

Figure 1. a, Representative images of synchrotron radiation microangiography (SRM) 5 days after PBS, CD34−, or CD34+ cell transplantation (pre sodium nitroprusside [SNP]; 7.0×7.0 mm). Collateral vessels were poorly visualized in all groups. Arrowhead shows ligation point (scale bar; 100 μm). b, Representative SRM images post SNP at day 5 (7.0×7.0 mm). Collateral vessels were poorly visualized in all groups (scale bar: 100 μm). c, Rentrop score of collateral development pre and post SNP in each group at day 5. d, Angiographic microvessel density (AMVD) pre and post SNP in each group at day 5. e, Ratio of AMVD post SNP to pre SNP (AMVD ratio) in each group at day 5.

SRM post SNP was similarly performed to evaluate the augmentation of new microvasculature 5 and 28 days after transplantation. SRM on day 5 revealed slightly better visualization of the new microvasculature post SNP compared with pre SNP in each group (Figure 1b). However, Rentrop score post SNP at day 5 was not significantly different in each group (Figure 1c). SRM on day 28 in CD34+ cell group, not in CD34− and PBS groups, revealed that new microvasculature in the occluded LAD area was better visualized post SNP than pre SNP (Figure 2a and 2b). Rentrop score at day 28 in CD34+ cell group was significantly greater post SNP than pre SNP (CD34+ post SNP, 1.8±0.1; CD34+ pre SNP, 1.6±0.2, $P<0.05$). However, in PBS or CD34− cell group, Rentrop score at day 28 post SNP was not significantly different from that pre SNP (Figure 2c).

SRM post SNP at day 28 revealed better visualization of collateral vessels into the distal LAD area in CD34+ cell group compared with both CD34− cell and PBS groups (Figure 2b). Rentrop score post SNP at day 28 was significantly greater in CD34+ cell group than either CD34− cell or PBS group (CD34+, 1.8±0.1; CD34−, 0.7±0.2; PBS, 0.5±0.2, $P<0.01$ for CD34+ versus CD34− and PBS) (Figure 2c).

Thus, the new generation SRM system enabled visualization and evaluation of new microvasculature created by CD34+ cell transplantation in the fast beating rat hearts. These results suggest that CD34+ cell transplantation may enhance collateral blood flow in the ischemic myocardium and may also improve collateral vascular function in response to SNP infusion.

Angiographic Microvessel Density (AMVD) in SRM

To quantify the activity of collateral vascular formation in the occluded LAD area, we measured the AMVD in SRM by computed analysis. AMVD pre and post SNP on day 5 was not significantly different in CD34+ cell group from that in other groups (Figure 1d). The ratio of AMVD post SNP to pre SNP (AMVD ratio) on day 5 was similar in all groups (Figure 1e).

AMVD pre SNP on day 28 was not significantly different in CD34+ cell group from that in other groups (CD34+, 27.3±3.2; CD34−, 23.2±0.8, PBS, 21.6±2.7). However, in CD34+ cell group, not in other groups, AMVD on day 28 was significantly greater post SNP than

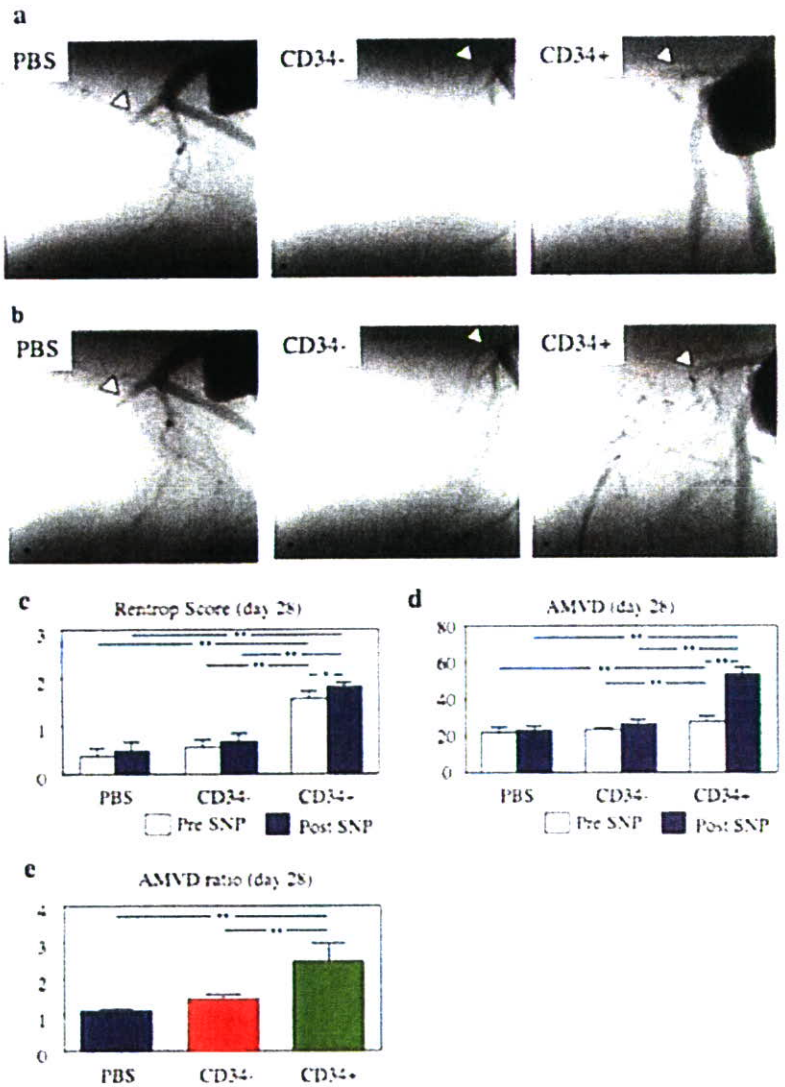

Figure 2. a, Representative microangiographic images pre SNP 28 days after PBS, CD34−, or CD34+ cell transplantation (7.0×7.0 mm). Collateral vessels were better developed in rat receiving CD34+ cells compared with rats receiving PBS and CD34− cells (scale bar, 100 μm). b, Representative microangiographic images post SNP at day 28 (7.0×7.0 mm). Augmentation of collateral microvessel development into distal portion of LAD area was further visualized in rat receiving CD34+ cells compared with rats receiving PBS and CD34− cells (scale bar, 100 μm). c, Rentrop score pre and post SNP at day 28 in each group. *$P<0.05$; **$P<0.01$. d, AMVD pre and post SNP at day 28 in each group. **$P<0.01$. e, AMVD ratio at day 28 in each group. **$P<0.01$.

pre SNP (post SNP, 53.2±3.8; pre SNP, 27.3±3.2, $P<0.05$). AMVD post SNP on day 28 was significantly greater in CD34+ cell group compared with CD34− cell and PBS groups (CD34+, 53.2±3.8; CD34−, 26.5±2.0, PBS, 23.0±2.0, $P<0.01$ for CD34+ versus CD34− and PBS) (Figure 2d). AMVD ratio on day 28 was also significantly greater in CD34+ cell group than either CD34− cell or PBS group (CD34+, 2.5±0.5; CD34−, 1.4±0.1, PBS, 1.1±0.1, $P<0.01$ for CD34+ versus CD34− or PBS). AMVD ratio on day 28 was similar in CD34− cell and PBS groups (Figure 2e).

These results indicate that AMVD analysis may be useful to quantify the effect of therapeutic neovascularization by CD34+ cell transplantation. Similarly as the Rentrop grade examination, AMVD assessment suggests contribution of CD34+ cell transplantation to improvement of collateral vessel function in response to SNP.

Histological Evaluation of Capillary Density

Histochemical staining for isolectin B4 was performed to identify capillaries in ischemic myocardium 4 weeks after cell transplantation (Figure 3a). Histological capillary density was significantly greater in CD34+ cell group than in CD34− cell and PBS groups. Histological capillary density in CD34− cell group was not significantly different from that in PBS group (CD34+, 711±15; CD34−, 365±23; PBS, 294±17/mm^2, $P<0.01$ for CD34+ versus CD34− and PBS) (Figure 3b).

Correlation Between SRM and Histological Assessments

To confirm whether AMVD is precise assessment of vascular development by CD34+ cell transplantation, we investigated correlation between AMVD and histological capillary density on day 28. AMVD pre SNP did not significantly correlate with histological capillary density ($R=0.16$, $P=0.42$), however AMVD post SNP closely correlated with histological capillary density ($R=0.82$, $P<0.0001$) (Figure 3c).

These results suggest that AMVD post SNP may be accurate and useful for precise evaluation of collateral and vascular formation following SCTx.

Discussion

Many investigators have demonstrated efficacy of various stem/progenitor cell transplantation against ischemic disease

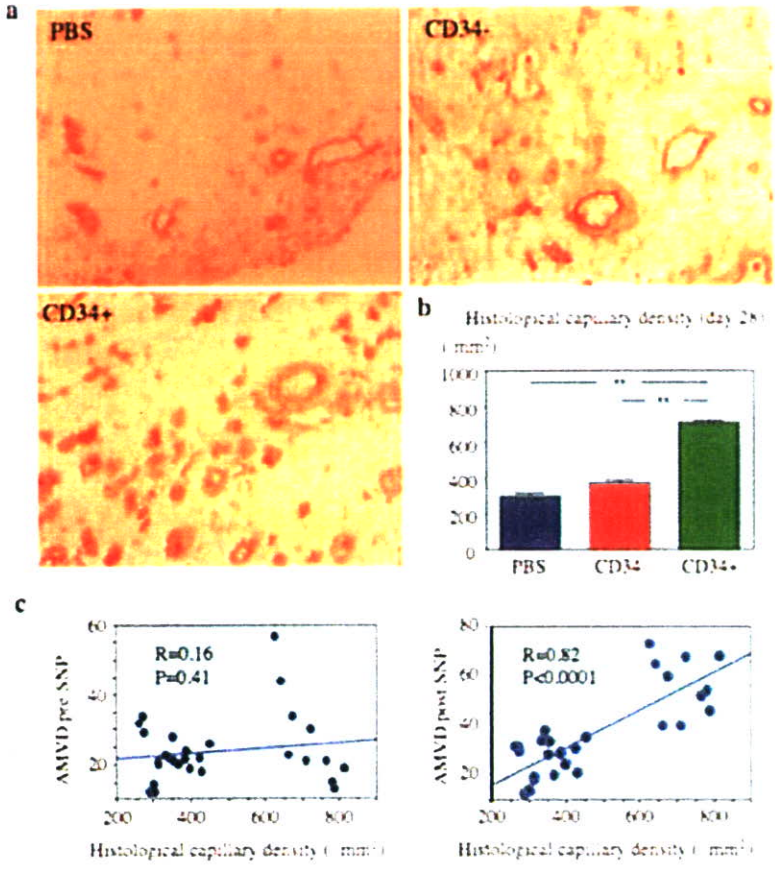

Figure 3. Histological and physiological evaluation of myocardial neovascularization after MI. a, Representative immunostaining for isolectin B4 in each group at day 28 (×200). b, Histological capillary density in rats receiving CD34+ cells, CD34− cells, or PBS at day 28. Ischemic neovascularization was significantly enhanced after CD34+ cell transplantation. $^{**}P<0.01$. c, Correlations of AMVD pre SNP or post SNP with histological capillary density 4weeks after the treatment. AMVD post SNP, but not pre SNP, closely correlated with histological capillary density.

such as MI and limb ischemia in vivo.[30,31] Although immunodeficient rats/mice provide enormous information about regenerative property of human stem/progenitor cells in the animal models of tissue ischemia, the vasculogenic/angiogenic effect of the human cells has been mainly evaluated by histological assessments because of technical limitation for physiological examinations in small animals.[15] Recently, Toyota et al[32] reported critical role of VEGF for coronary collateral growth by using micro CT. However, the micro CT can be performed only for postmortem examination, ie, not for fast beating hearts, and the spatial resolution of this method was 18 μm, which is 3 times larger than that in our novel SRM system and is not considered to be ideal for visualization of the collateral vessels.

In our SRM system, monochromatic SR is used as an x-ray source, and high speed and resolution imaging system, which has the potential to visualize blood vessels as small as 20 μm in diameter (spatial resolution: 6 μm), is also used. In the present study, we demonstrated usefulness of the SRM imaging to evaluate therapeutic neovascularization by cell-based therapy in small animals. Similarly as the previous reports,[4,7,8] histological and molecular examinations in this study confirmed endothelial differentiation and therapeutic efficacy of the transplanted CD34+ cells for augmentation of myocardial neovascularization. The SRM examination revealed that diameter of the collateral vessels was generally 20 to 120 μm, which is apparently invisible size in conventional angiography, and the collaterals were better visualized after SNP-induced vasodilatation than pre SNP. In comparison with postmortem studies such as histology, corrosion casts infusion and micro CT, it may be a great advantage of the SRM to elucidate physiology of the microvessels in response to vasoactive agents under the fast beating condition. To our knowledge, this is the first report demonstrating coronary microangiography under fast beating condition in both acute and chronic phases after MI and SCTx. Extent of collateral development was evaluated by conventional Rentrop score and novel assessment of AMVD. Although Rentrop score has been widely used in preclinical and clinical fields,[7] the examination has several limitations: (1) The scoring is semi-quantitative; (2) The system is to indirectly evaluate collateral development by grading collateral filling into the occluded coronary artery, and not to directly examine developed vascularization. Therefore, we assessed AMVD to quantitatively and directly evaluate blood vessel development as angiographic vessel density independent of blood flow in the occluded arteries. In the present study, both conventional and novel assessments revealed that collateral development and vascularization in ischemic myocardium was similar in all groups on day 5, but was significantly augmented in CD34+ cell group than other groups on day 28. Interestingly, the intergroup difference in AMVD was observed only post SNP, not pre SNP. Similarly, AMVD post SNP, not pre SNP, closely correlated with histological capillary density, which has been used for morphological evaluation of neovascularization in small animal studies. These results indicate accuracy and usefulness of AMVD post SNP for elucidating preserved vascular volume created by SCTx in fast beating

hearts of small animals, and also suggest that even in SRM with high imaging resolution, SNP infusion may be essential to avoid underestimation of the angiographic vascular density. The correlation between histological capillary density and AMVD post SNP proves the quality of AMVD to identify capillary vascular volume regenerated by SCTx. SNP infusion may increase the diameter of not only already visible vessels but also invisible capillaries (diameter <20 μm) pre SNP up to detectable size, thereby represents significant augmentation of blood perfusion in ischemic myocardium following CD34+ cell transplantation.

Present Limitations and Future Plans

The microangiographic imaging system requires a high shutter speed (short exposure time) to produce sharp and blur-free images of fast-moving hearts. In the current SRM system, the rotating disk X-ray shutter has been developed to produce X-ray pulses with the minimum pulse length of 0.1 ms, because even the beating heart is to remain almost motionless during the exposure time for ideal imaging. However, the exposure time was adjusted to around 2.0 ms in this experiment, because X-ray flux was not sufficient for the 0.1 ms shutter operation. A speed of the coronary arteries in rats is a few μm/ms at the end of diastole, ie, the movement of the arteries in 2.0 ms is several μm in the present system. On the other hand, the limiting spatial resolution of the image detector is approximately 6 μm, when digital images are acquired with a 1024×1024 pixel format, an input field of view of 4.5 mm×4.5 mm and pixel size of 4.5 μm. These facts indicate that the detector's spatial resolution is comparable to the motion blur amount in the present rat heart imaging, however there is still some room for improvement of the image quality. We are planning to develop a new X-ray optical system used for SR to increase the X-ray flux for the 0.1 ms shutter operation. Another limitation of the present study is that despite of the high quality of SRM for visualization of coronary arteries and the microvascular bed of fast beating hearts, we cannot take serial images in each individual at days 5 and 28, because they have to be examined ex vivo not in vivo. Future establishment of in vivo SRM imaging would be also warranted.

Conclusions

The present results indicate that the SRM may be useful to both morphologically and physiologically evaluate therapeutic neovascularization by SCTx in small animals. The novel imaging system may be not only an essential tool in future translational research of stem cell biology but also useful assessment of microvascular beds in small animal models of various diseases such as hypertension, diabetes mellitus, and cardiomyopathy. Further development of in vivo imaging system in future may lead to clinical application of the SRM, which is expected to be useful for assessment of microangiopathy, elucidation of therapeutic neovascularization, and determination of optimal treatment strategies in both preclinical and clinical trials.

Acknowledgments

We thank Yumiko Masukawa and Tomoko Iioh for their secretarial assistance. The synchrotron radiation experiments were performed at the BL28B2 in the SPring-8 with the approval of the Japan Synchrotron Radiation Research Institute (Proposal Nos. 2004B0339 and 2005A0590).

Sources of Funding

This work was supported by Health and Labor Sciences Research Grants (H14-trans-001, H17-trans-002) from Japanese Ministry of Health, Labor, and Welfare.

Disclosures

None.

References

1. Freedman SB, Isner JM. Therapeutic angiogenesis for coronary artery disease. *Ann Intern Med.* 2002;136:54–71.
2. Losordo DW, Vale PR, Hendel RC, Milliken CE, Fortuin FD, Cummings N, Schatz RA, Asahara T, Isner JM, Kuntz RE. Phase 1/2 placebo-controlled, double-blind, dose-escalating trial of myocardial vascular endothelial growth factor 2 gene transfer by catheter delivery in patients with chronic myocardial ischemia. *Circulation.* 2002;105:2012–2018.
3. Menasche P, Hagege AA, Scorsin M, Pouzet B, Desnos M, Duboc D, Schwartz K, Vilquin JT, Marolleau JP. Myoblast transplantation for heart failure. *Lancet.* 2001;357:279–280.
4. Kocher AA, Schuster MD, Szabolcs MJ, Takuma S, Burkhoff D, Wang J, Homma S, Edwards NM, Itescu S. Neovascularization of ischemic myocardium by human bone-marrow-derived angioblasts prevents cardiomyocyte apoptosis, reduces remodeling and improves cardiac function. *Nat Med.* 2001;7:430–436.
5. Asahara T, Murohara T, Sullivan A, Silver M, van der Zee R, Li T, Witzenbichler B, Schatteman G, Isner JM. Isolation of putative progenitor endothelial cells for angiogenesis. *Science.* 1997;275:964–967.
6. Asahara T, Masuda H, Takahashi T, Kalka C, Pastore C, Silver M, Kearne M, Magner M, Isner JM. Bone marrow origin of endothelial progenitor cells responsible for postnatal vasculogenesis in physiological and pathological neovascularization. *Circ Res.* 1999;85:221–228.
7. Kawamoto A, Tkebuchava T, Yamaguchi J, Nishimura H, Yoon YS, Milliken C, Uchida S, Masuo O, Iwaguro H, Ma H, Hanley A, Silver M, Kearney M, Losordo DW, Isner JM, Asahara T. Intramyocardial transplantation of autologous endothelial progenitor cells for therapeutic neovascularization of myocardial ischemia. *Circulation.* 2003;107:461–468.
8. Iwasaki H, Kawamoto A, Ishikawa M, Oyamada A, Nakamori S, Nishimura H, Sadamoto K, Horii M, Matsumoto T, Murasawa S, Shibata T, Suehiro S, Asahara T. Dose-dependent contribution of CD34-positive cell transplantation to concurrent vasculogenesis and cardiomyogenesis for functional regenerative recovery after myocardial infarction. *Circulation.* 2006;113:1311–1325.
9. Kawamoto A, Gwon HC, Iwaguro H, Yamaguchi JI, Uchida S, Masuda H, Silver M, Ma H, Kearney M, Isner JM, Asahara T. Therapeutic potential of ex vivo expanded endothelial progenitor cells for myocardial ischemia. *Circulation.* 2001;103:634–637.
10. Kemp PA, Gardiner SM, March JE, Rubin PC, Bennett T. Assessment of the effects of endothelin-1 and magnesium sulphate on regional blood flows in conscious rats, by the coloured microsphere reference technique. *Br J Pharmacol.* 1999;126:621–626.
11. Conrad MC, Anderson JL 3rd, Garrett JB Jr. Chronic collateral growth after femoral artery occlusion in the dog. *J Appl Physiol.* 1971;31:550–555.
12. Verheyen A, Vlaminckx E, Lauwers F, Van Den Broeck C, Wouters L. Serotonin-induced blood flow changes in the rat hindlegs after unilateral ligation of the femoral artery. Inhibition by the S2 receptor antagonist ketanserin. *Arch Int Pharmacodyn Ther.* 1984;270:280–298.
13. Orlandi C, Blackshear JL, Hollenberg NK. Specific increase in sensitivity to serotonin of the canine hindlimb collateral arterial tree via the 5-hydroxytryptamine-2 receptor. *Microvasc Res.* 1986;32:121–130.
14. Takeshita S, Zheng LP, Brogi E, Kearney M, Pu LQ, Bunting S, Ferrara N, Symes JF, Isner JM. Therapeutic angiogenesis. A single intraarterial bolus of vascular endothelial growth factor augments revascularization in a rabbit ischemic hind limb model. *J Clin Invest.* 1994;93:662–670.
15. Mori H, Hyodo K, Tobita K, Chujo M, Shinozaki Y, Sugishita Y, Ando M. Visualization of penetrating transmural arteries in situ by monochromatic synchrotron radiation. *Circulation.* 1994;89:863–871.
16. Mori H, Hyodo K, Tanaka E, Uddin-Mohammed M, Yamakawa A, Shinozaki Y, Nakazawa H, Tanaka Y, Sekka T, Iwata Y, Handa S,

Umetani K, Ueki H, Yokoyama T, Tanioka K, Kubota M, Hosaka H, Ishikawa N, Ando M. Small-vessel radiography in situ with monochromatic synchrotron radiation. *Radiology*. 1996;201:173–177.
17. White FC, Carroll SM, Magnet A, Bloor CM. Coronary collateral development in swine after coronary artery occlusion. *Circ Res*. 1992;71:1490–1500.
18. Unger EF, Banai S, Shou M, Lazarous DF, Jaklitsch MT, Scheinowitz M, Correa R, Klingbeil C, Epstein SE. Basic fibroblast growth factor enhances myocardial collateral flow in a canine model. *Am J Physiol*. 1994;266:H1588–1595.
19. Takeshita S, Rossow ST, Kearney M, Zheng LP, Bauters C, Bunting S, Ferrara N, Symes JF, Isner JM. Time course of increased cellular proliferation in collateral arteries after administration of vascular endothelial growth factor in a rabbit model of lower limb vascular insufficiency. *Am J Pathol*. 1995;147:1649–1660.
20. Rubenstein E, Hofstadter R, Zeman HD, Thompson AC, Otis JN, Brown GS, Giacomini JC, Gordon HJ, Kernoff RS, Harrison DC, et al. Transvenous coronary angiography in humans using synchrotron radiation. *Proc Natl Acad Sci U S A*. 1986;83:9724–9728.
21. Mori H, Tanaka E, Hyodo K, Uddin Mohammed M, Sekka T, Ito K, Shinozaki Y, Tanaka A, Nakazawa H, Abe S, Handa S, Kubota M, Tanioka K, Umetani K, Ando M. Synchrotron microangiography reveals configurational changes and to-and-fro flow in intramyocardial vessels. *Am J Physiol*. 1999;276:H429–H437.
22. Takeshita S, Isshiki T, Mori H, Tanaka E, Eto K, Miyazawa Y, Tanaka A, Shinozaki Y, Hyodo K, Ando M, Kubota M, Tanioka K, Umetani K, Ochiai M, Sato T, Miyashita H. Use of synchrotron radiation microangiography to assess development of small collateral arteries in a rat model of hindlimb ischemia. *Circulation*. 1997;95:805–808.
23. Tanaka E, Tanaka A, Sekka T, Shinozaki Y, Hyodo K, Umetani K, Mori H. Digitized cerebral synchrotron radiation angiography: quantitative evaluation of the canine circle of Willis and its large and small branches. *Am J Neuroradiol*. 1999;20:801–806.
24. Sekka T, Volchikhina SA, Tanaka A, Hasegawa M, Tanaka Y, Ohtani Y, Tajima T, Makuuchi H, Tanaka E, Iwata Y, Sato S, Hyodo K, Ando M, Umetani K, Kubota M, Tanioka K, Mori H. Visualization, quantification and therapeutic evaluation of angiogenic vessels in cancer by synchrotron microangiography. *J Synchrotron Radiat*. 2000;7:361–367.
25. Kidoguchi K, Tanaki M, Mizobe T, Koyama J, Kondoh T, Kohmura E, Sakurai T, Yokono K, Umetani K. In vivo X-ray angiography in the mouse brain using synchrotron radiation. *Stroke*. 2006;37:1856–1861.
26. Gaipa G, Dassi M, Perseghin P, Venturi N, Corti P, Bonanomi S, Balduzzi A, Longoni D, Uderzo C, Biondi A, Masera G, Parini R, Bertagnolio B, Uziel G, Peters C, Rovelli A. Allogeneic bone marrow stem cell transplantation following CD34+ immunomagnetic enrichment in patients with inherited metabolic storage diseases. *Bone Marrow Transplant*. 2003;31:857–860.
27. Beaussier M, Mouren S, Souktani R, Arthaud M, Massias L, Vicaut E, Lienhart A, Coriat P. Role of nitric oxide and cyclooxygenase pathways in the coronary vascular effects of halothane, isoflurane and desflurane in red blood cell-perfused isolated rabbit hearts. *Br J Anaesth*. 2002;88:399–407.
28. Heitzer T, Baldus S, von Kodolitsch Y, Rudolph V, Meinertz T. Systemic endothelial dysfunction as an early predictor of adverse outcome in heart failure. *Arterioscler Thromb Vasc Biol*. 2005;25:1174–1179.
29. Becker A, Reith A, Napiwotzki J, Kadenbach B. A quantitative method of determining initial amounts of DNA by polymerase chain reaction cycle titration using digital imaging and a novel DNA stain. *Anal Biochem*. 1996;237:204–207.
30. Orlic D, Kajstura J, Chimenti S, Jakoniuk I, Anderson SM, Li B, Pickel J, McKay R, Nadal-Ginard B, Bodine DM, Leri A, Anversa P. Bone marrow cells regenerate infarcted myocardium. *Nature*. 2001;410:701–705.
31. Jackson KA, Majka SM, Wang H, Pocius J, Hartley CJ, Majesky MW, Entman ML, Michael LH, Hirschi KK, Goodell MA. Regeneration of ischemic cardiac muscle and vascular endothelium by adult stem cells. *J Clin Invest*. 2001;107:1395–1402.
32. Toyota E, Warltier DC, Brock T, Ritman E, Kolz C, O'Malley P, Rocic P, Focardi M, Chilian WM. Vascular endothelial growth factor is required for coronary collateral growth in the rat. *Circulation*. 2005;112:2108–2113.

Estrogen-Mediated Endothelial Progenitor Cell Biology and Kinetics For Physiological Postnatal Vasculogenesis

Haruchika Masuda, Christoph Kalka, Tomono Takahashi, Miyoko Yoshida, Mika Wada, Michiru Kobori, Rie Itoh, Hideki Iwaguro, Masamichi Eguchi, Yo Iwami, Rica Tanaka, Yoshihiro Nakagawa, Atsuhiko Sugimoto, Sayaka Ninomiya, Shinichiro Hayashi, Shunichi Kato, Takayuki Asahara

Abstract—Estrogen has been demonstrated to promote therapeutic reendothelialization after vascular injury by bone marrow (BM)–derived endothelial progenitor cell (EPC) mobilization and phenotypic modulation. We investigated the primary hypothesis that estrogen regulates physiological postnatal vasculogenesis by modulating bioactivity of BM-derived EPCs through the estrogen receptor (ER), in cyclic hormonally regulated endometrial neovascularization. Cultured human EPCs from peripheral blood mononuclear cells (PB-MNCs) disclosed consistent gene expression of ER α as well as downregulated gene expressions of ER β. Under the physiological concentrations of estrogen (17β-estradiol, E2), proliferation and migration were stimulated, whereas apoptosis was inhibited on day 7 cultured EPCs. These estrogen-induced activities were blocked by the receptor antagonist, ICI182,780 (ICI). In BM transplanted (BMT) mice with ovariectomy (OVX) from transgenic mice overexpressing β-galactosidase (lacZ) regulated by an endothelial specific Tie-2 promoter (Tie-2/lacZ/BM), the uterus demonstrated a significant increase in BM-derived EPCs (lacZ expressing cells) incorporated into neovasculatures detected by CD31 immunohistochemistry after E2 administration. The BM-derived EPCs that were incorporated into the uterus dominantly expressed ER α, rather than ER β in BMT mice from BM of transgenic mice overexpressing EGFP regulated by Tie-2 promoter with OVX (Tie-2/EGFP/BMT/OVX) by ERs fluorescence immunohistochemistry. An in vitro assay for colony forming activity as well as flow cytometry for CD133, CD34, KDR, and VE-cadherin, using human PB-MNCs at 5 stages of the female menstrual-cycle (early-proliferative, pre-ovulatory, post-ovulatory, mid-luteal, late-luteal), revealed cycle-specific regulation of EPC kinetics. These findings demonstrate that physiological postnatal vasculogenesis involves cyclic, E2-regulated bioactivity of BM-derived EPCs, predominantly through the ERα. (*Circ Res.* **2007;101:598-606.**)

Key Words: estrogen ■ endothelial progenitor cell ■ estrogen receptor ■ physiological postnatal vasculogenesis

In the female reproductive system, neovascularization is a recurring phenomemnon controlled by cyclic development of transient structure and cyclical repair of damaged tissue.[1] The ovarian sex steroid hormones, estrogen and progesterone, are primarily uterotropic and control the cyclical patterns of uterine cell proliferation and vascular growth that occur throughout the nonpregnant menstrual cycle. Given the synchronized nature of neovascularization in this cyclical mannter, it is assumed that angiogenic growth factor expression is induced by steroid hormones and regulates blood vessel formation in reproductive organogenesis.[2-5]

Despite clinical evidence for the significant role of steroid hormones in endometrial neovascularization, further investigation using in vitro and in vivo experiments have yielded inconclusive results regarding pathophysiological mechanisms in angiogenesis.[6-10] Moreover, estrogen has been shown to exhibit an inhibitory effect on certain hematopoietic kinetics, including lymphocytes and monocytes, both in terms of number and function.[11-14] Endometrial vascularization has formerly been considered to develop via "angiogenesis", ie, proliferation and migration of fully differentiated endothelial cells (ECs) from preexisting "parent" vessels.[15] However, circulating EPCs have been shown to incorporate into foci of neovascularization in adult species,[16] consistent with the notion of postnatal "vasculogenesis".[17] EPCs comprise of undifferentiated blood MNCs which are mobilized from BM by ischemic stimuli and angiogenic/hematopoietic factors,[17] and subsequently home to, differentiate, and proliferate in foci of neovascularization.[18]

Original received November 3, 2006; revision received June 11, 2007; accepted July 16, 2007.

From the Department of Regenerative Medicine (H.M., M.Y., M.W., M.K., R.I., H.I., M.E., Y.I., R.T., Y.N., A.S., S.N., S.K., T.A.), Tokai University School of Medicine, Isehara, Japan; the Department of Vascular Medicine (C.K.), Swiss Cardiovascular Center, University Hospital of Bern, Switzerland; the third Department of Internal Medicine (T.T.), Tokyo Medical University, Japan; the Department of Cell Signaling (S.H.), Gifu University Graduate School of Medicine, Japan.; Stem Cell Translational Research (T.A.), Institute of Biomedical Research and Innovation/ RIKEN Center for Developmental Biology, Kobe, Japan.

Correspondence to Takayuki Asahara, MD, PhD, Department of Regenerative Medicine, Tokai University School of Medicine, Bohseidai, Isehara, Kanagawa 259-1193, Japan. E-mail asa777@aol.com

Circulation Research is available at http://circres.ahajournals.org

DOI: 10.1161/CIRCRESAHA.106.144006

Given this new understanding of adult neovascularization, it is also possible that vasculogenesis could also be responsible for ovarian hormonal regulation of endometrial neovascularization. Recently, 2 groups have demonstrated promotive effect of estrogen on reendothelialization after vascular injury via EPC incorporation. Iwakura et al disclosed an NO-dependent estrogen effect on EPCs using eNOS KO mice,[19,20] and Strehlow et al indicated an estrogen dependent antiapoptotic effect on EPC biology. Hamada et al demonstrated the functional importance of ER expression by EPCs.[21] Together, these reports suggest a therapeutic application of altering estrogen levels directly, or its receptor agonists, for vascular repair.

Therefore, in the current study, we investigated the hypothesis that E2 regulates physiological neovascularization of the endometrium by modulating the biology and kinetics of BM-derived EPCs.

Methods

EPC Culture of Human and Mouse EPCs

Human and mouse EPCs were cultured by using a modified protocol that has previously been reported.[18,22,23] Phenol-red free (PRF) endothelial basal media (EBM, Clonetics) was used to delete estrogenic effect, as described in Supplementary Method (SM)-I, available online at http://circres.ahajournals.org.[24,25]

Effects of Estrogen on EPCs: Differentiation, Proliferation, Migration, and Antiapoptosis In Vitro

The assays for EPC bioactivity effected by E2 were performed, according to the detailed description in SM-II, as previously reported.[19,26]

RT-PCR for Endothelial Gene Expression in Cultured Human EPCs

The protocol for RT-PCR assay was described in SM-III.

Real Time PCR Assay for Gene Expression of Estrogen Receptors in Cultured Human EPCs

The protocol of real time PCR assay was described in SM-IV.

Mouse Cultured EPC Assay

The protocol of mouse cultured EPC assay was described in SM-V.[18,22,23]

Mouse Cornea Neovascularization Assay

The effect of E2-induced EPC kinetics on neovascularization was studied by E2 pretreated OVX mice for 4 days as described in SM-6.[18,22,27]

Study Design of BMT Animal Experiments

BMT animal models with endogenous sex hormone depletion were developed as follows: female nude SCID mice (NIHS-bg-nu-xid, Taconic, Albany, NY; 4 weeks) were lethally irradiated and received BM cells from age-matched female Tie-2 transgenic mice overexpressing β-galactosidase by Tie-2 promoter (FVB/N-TgN[TIE2LacZ]182Sato, Jackson Laboratory, Bar Harbor, Me).[17,22,28] The protocol of BMT animal experiments was depicted in SM-VII.

Cellular Identification of LacZ Expressing Cells in Uterus or Cornea of Tie-2/LacZ/BMT/OVX Mice

Uterus Experiments

The uterus of mice euthanized at day 2, day 4, and day 7 after subcutaneous E2 pellet implantation was processed for CD31 immunohistochemistry as well as LacZ staining,[17] as described in SM-VIII. LacZ positive cells in whole area, or localized in vascular wall or stroma per uterus tissue section were counted. The percentage of LacZ positive cells localized in each part versus whole area was assayed.

Cornea Experiments

Six days after making the cornea model, the cornea was observed, after staining eye balls with LacZ solution. LacZ stained tissues embedded in paraffin were processed to CD31 immunohistochemistry.

Investigation of ER α and ER β Expression by BM-Derived EPCs Incorporated Into the Uterus of Tie-2/EGFP/BMT/OVX Mice

The protocol was described in SM-IX.

EPC Culture Assay and Flow Cytometry in Menstrual Cycle of Premenopausal Women

EPC culture assay and flow cytometrical analysis were performed, using PB-MNCs of 6 healthy premenopausal females (aged 20 to 40) at 5 separate stages of the menstrual cycle: T1=early proliferative, T2=preovulatory, T3=postovulatory, T4=mid luteal, and T5=late luteal, as previously described.[29] Flow cytometrical analysis (FACS) was performed on a FACStar flow cytometer (Becton Dickinson) and a Cell Quest software (Becton Dickinson), as described in SM-X.

EPC Colony Forming Activity of PB in Menstrual Cycle of Premenopausal Women

EPC colony forming activity was also assessed by SM-XI and XII.

Notice on Experiments in Animal and Human Subjects

Notice on experiments in animal and human subjects was described in SM-XIII.

Statistical Analysis

All results are expressed as mean±SE. Statistical significance was evaluated using unpaired Student *t* test for the comparison between 2 groups and ANOVA followed by Fisher post hoc test for the comparison among multiple groups. A probability value less than 0.05 was interpreted to denote statistical significance.

Results

Quantitative Real Time PCR Assay of ER α and ER β Gene Expressions in Cultured Human EPCs

In day 7 cultured human EPCs, endothelial gene expressions of von Willbrand Factor (vWF) and CD31 were detected (Figure 1A). To establish the potential for a direct effect of E2 on EPCs, mRNA expression of ER α and ER β was assessed by quantitative real time PCR assay. The gene expressions of ER α and ER β in cultured EPCs varied during the culture period. The expression of ER α did not change between day 4 and day 7, whereas the expression of ER β was remarkably downregulated at day 7 to the level of 0.12 fold relative to day 4 (Figure 1B).

Receptor Mediated E2 Effects on EPC Activity

EPC bioactivities upregulated by E2 were deleted in the presence of ICI, suggesting the ER mediated bioactivities, as described in supplemental Figure (SF)-I.

Upregulation of EPC Kinetics After E2 Administration

To explore the systemic effects of E2 on EPC kinetics, we administered E2 to OVX female and CST male mice. The

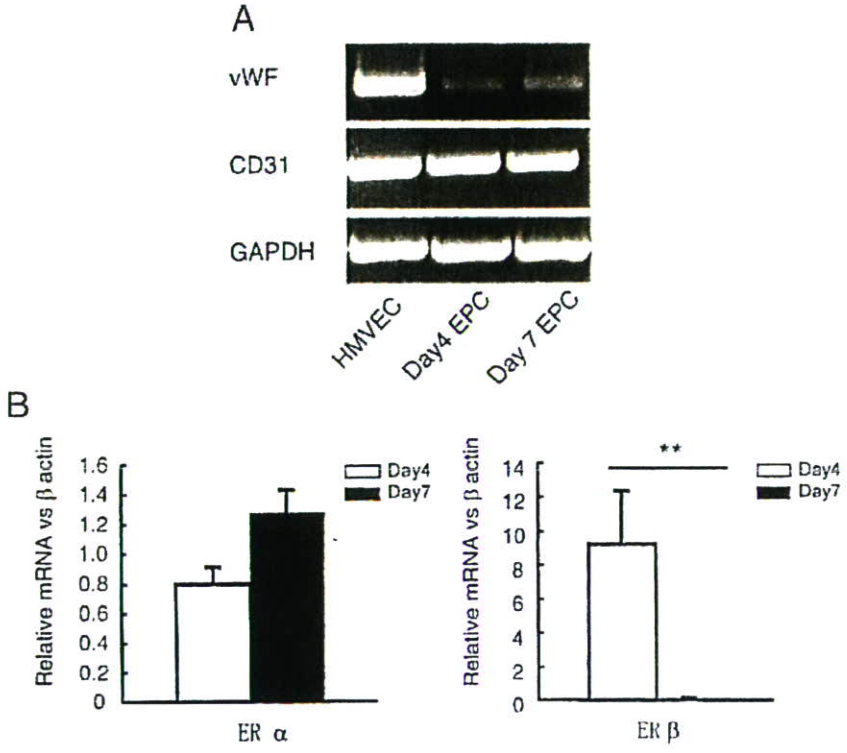

Figure 1. Quantitative real-time PCR assay of ERs gene expressions in cultured human EPCs. A, Endothelial gene expressions of vWF and CD31 in cultured human EPCs supplied for in vitro experiments. HMVECs, human microvascular ECs served as a positive control. B, Quantitative real-time PCR assay of ERs gene expressions in cultured human EPCs. The assay was performed on 3 human subjects. The analysis was performed using ddCt method. dCt values of ERs vs β-actin from each Ct value were acquired at each time point. ddCt values at each time point on each ER were calculated from each dCt value at day 4 or day 7. Relative mRNA vs β-actin presents $2^{(-ddCt)}$, n=3, $^{**}p<0.01$.

EPC culture assay[22] revealed a significant increase in endothelial lineage cells in cultures of PB-MNCs isolated at 2 to 4 days after subcutaneous implantation of E2 pellet in both OVX and CST mice. EPCs, identified by acLDL-DiI uptake and BS-1 lectin- FITC reactivity, consisted principally of spindle-shaped cells, often forming colonies. The number of cultured EPCs decreased to or below the level of pre-implantation by day 7 (Figure 2A and 2B). In controls, pellet implant did not increase EPC numbers significantly. These results thus provide quantitative evidence that E2 mobilizes EPCs from BM into the peripheral circulation.

Enhanced Cornea Neovascularization After E2 Administration

Examination of the cornea in E2- or P-treated mice established the extent of vascular development induced by implantation of a VEGF-containing pellet in the mouse cornea, presented in SF-II.

Identification of BM-Derived EPCs Within the Endometrium of Tie-2/LacZ/BMT/OVX Mice After E2 Administration

Before pellet implantation, macroscopic examination of the uterus of Tie-2/LacZ/BMT/OVX mice from both groups

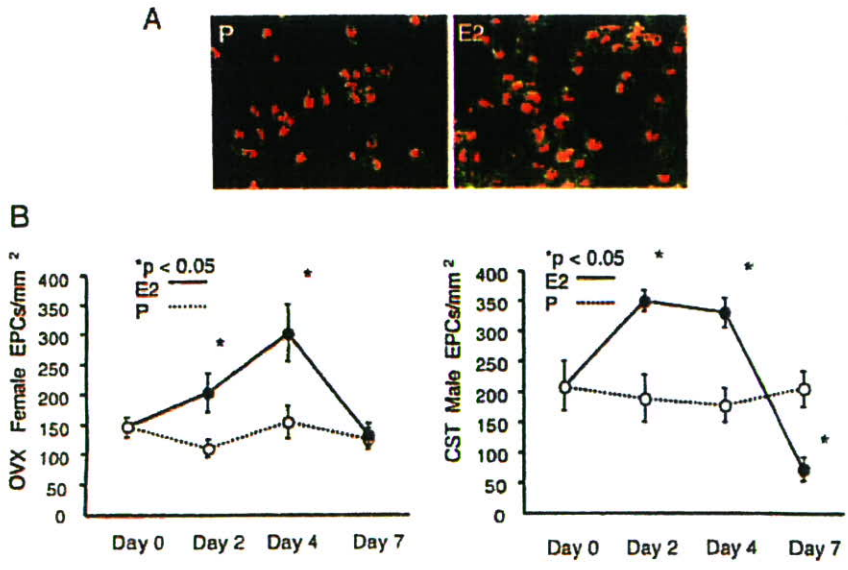

Figure 2. EPC culture assay in mice after E2 administration. A, Representative fluorescent photomicrographs of cultured EPCs merged acLDL- DiI with BS-1 lectin-FITC at day 4 in P and E2 treated OVX female mouse. ×10 magnification. B, Time course of EPC frequency in culture of PB-MNCs from E2- or P- treated mice. The results are shown for both OVX and CST mice, n=6 mice /each group.

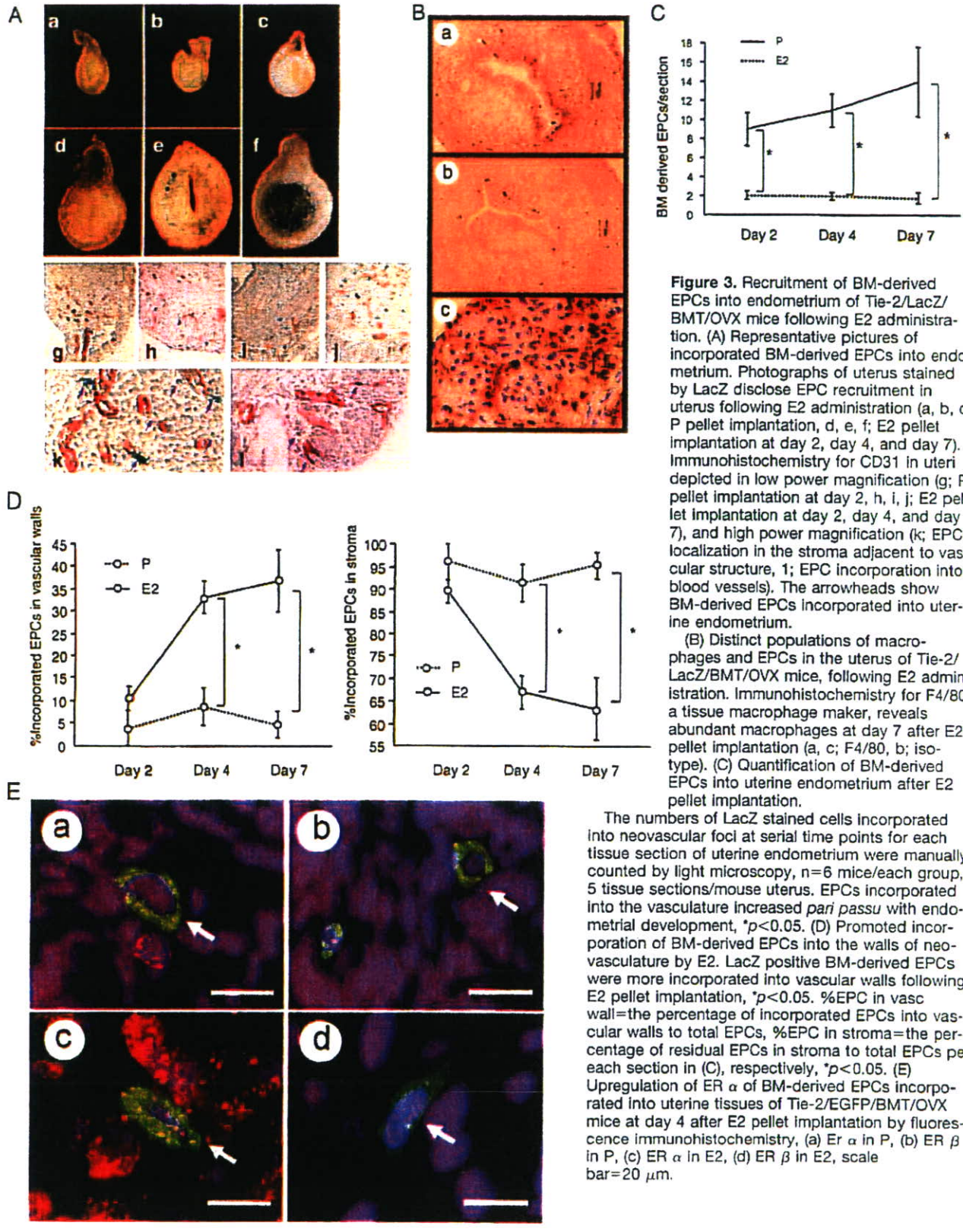

Figure 3. Recruitment of BM-derived EPCs into endometrium of Tie-2/LacZ/BMT/OVX mice following E2 administration. (A) Representative pictures of incorporated BM-derived EPCs into endometrium. Photographs of uterus stained by LacZ disclose EPC recruitment in uterus following E2 administration (a, b, c; P pellet implantation, d, e, f; E2 pellet implantation at day 2, day 4, and day 7). Immunohistochemistry for CD31 in uteri depicted in low power magnification (g; P pellet implantation at day 2, h, i, j; E2 pellet implantation at day 2, day 4, and day 7), and high power magnification (k; EPC localization in the stroma adjacent to vascular structure, 1; EPC incorporation into blood vessels). The arrowheads show BM-derived EPCs incorporated into uterine endometrium.

(B) Distinct populations of macrophages and EPCs in the uterus of Tie-2/LacZ/BMT/OVX mice, following E2 administration. Immunohistochemistry for F4/80, a tissue macrophage maker, reveals abundant macrophages at day 7 after E2 pellet implantation (a, c; F4/80, b; isotype). (C) Quantification of BM-derived EPCs into uterine endometrium after E2 pellet implantation.

The numbers of LacZ stained cells incorporated into neovascular foci at serial time points for each tissue section of uterine endometrium were manually counted by light microscopy, n=6 mice/each group, 5 tissue sections/mouse uterus. EPCs incorporated into the vasculature increased *pari passu* with endometrial development, $^*p<0.05$. (D) Promoted incorporation of BM-derived EPCs into the walls of neovasculature by E2. LacZ positive BM-derived EPCs were more incorporated into vascular walls following E2 pellet implantation, $^*p<0.05$. %EPC in vasc wall=the percentage of incorporated EPCs into vascular walls to total EPCs, %EPC in stroma=the percentage of residual EPCs in stroma to total EPCs per each section in (C), respectively, $^*p<0.05$. (E) Upregulation of ER α of BM-derived EPCs incorporated into uterine tissues of Tie-2/EGFP/BMT/OVX mice at day 4 after E2 pellet implantation by fluorescence immunohistochemistry, (a) Er α in P, (b) ER β in P, (c) ER α in E2, (d) ER β in E2, scale bar=20 μm.

disclosed occasional blue LacZ-stained cells located mainly in the mesometrium. In mice with P pellet implants, the uterus remained atrophic, and the location and frequency of LacZ-stained BM-derived EPCs did not change during observation. In contrast, Tie-2/LacZ/BMT/OVX mice with implanted E2 pellet revealed an evolving pattern of BM-derived, LacZ-positive cells within the uterus. Two days after E2 pellet implant, the frequency of LacZ-positive cells increased

throughout the uterus but remained concentrated in the outer layer of myometrium. By day 4 after implantation, EPCs continued to increase in number and were now identified in the outer and inner layers of myometrium and endometrium. EPCs finally accumulated in large numbers within the endometrium 7 days after E2 implantation. Immunohistochemical staining for CD31 in the P group demonstrated LacZ-stained CD31-positive EPCs appearing as round cells localized in the stroma adjacent to established vessels and incorporated as spindle-shaped cells into vascular walls. After E2 pellet implantation, EPCs were more frequently found to be incorporated within the vascular walls of the endometrium (Figure 3A). Counterstaining with antibody F4/80, as a tissue macrophage marker, and LacZ staining, revealed that the macrophages did not express β-gal; thereby indicating that they do not express Tie-2 and are therefore a completely separate population from the EPCs identified by Tie-2 promoter driven LacZ expression (Figure 3B). EPCs incorporation into foci of uterine neovascularization increased significantly by approximately 4.5-, 5.5-, or 7.8-fold at day 2, day 4, or day 7 after E2 pellet implantation versus endometrial tissues harvested from P pellet implants examined at identical time points. The number of incorporated EPCs per uterine section were as follows: for E2 group, day 2=9.0±1.8, day 4=11.0±1.7, day 7=14.0±3.6; in contrast, for P group, day 2=2.1±0.4, day 4=2.0±0.3, and day 7=1.8±0.5 (Figure 3C). Also, after E2 pellet implantation, the percentage of BM-derived EPCs incorporated into the neovasculature (of the total BM-derived EPCs per uterine section) increased significantly (day 2=10.44±2.7%, day 4=33.01±3.7%, day 7=36.73±6.9%); in contrast, the percentage for P group remained low (day 2=3.85±3.8%, day 4=8.56±4.1%, and day 7=4.44±2.9%; Figure 3D). On the other hand, the percentage of BM-derived EPCs in the stroma of the E2 group decreased inversely (day 2=89.57±2.7%, day 4=66.99±3.7%, day 7=63.27±6.9%), whereas the percentage for P group remained high (day 2=96.15±3.8%, day 4=91.44±4.1%, and day 7=95.56±2.9%; Figure 3D).

These findings indicate that BM-derived EPCs incorporate into foci of neovascularization during E2-induced endometrial maturation. This effect was restricted to E2-responsive organs: incorporated EPCs in other organs such as lung, liver, or skin,[17] could not be enhanced by E2 (data not shown). The sequence of histologic patterns observed suggests that E2 mobilizes BM-derived EPCs via the circulation (vide infra) into the myometrium from mesometrium, which precedes accumulation and incorporation into the neovasculature of the endometrium. The representative feature of BM-derived EPC incorporation into endothelial layer of vessel wall in uterine endometrium was recognized at day 7 after E2 pellet implantation by fluorescence immunohistochemistry of EGFP cellular positivity in CD31 positive endothelial layer (SF-III).

BM-derived EPCs (Tie-2/EGFP positive cells) incorporated into uterine tissues in Tie-2/EGFP/BMT/OVX mice, expressing ER α by stimulation of E2 pellet implantation for 4 days, but not ER β by fluorescence immunohistochemistry (Figure 3E). In this context, it is intriguing to note that the pattern of EPC recruitment and incorporation is identical to the previously established pattern of in situ VEGF expression in the hormone-regulated cycle of endometrial development and regression.[3]

Recruitment of BM-Derived EPCs into Cornea Neovascularization of Tie-2/LacZ/BMT/OVX Mice Following E2 Administration

Macroscopically, BM-derived EPCs stained with LacZ were observed more frequently in cornea of E2 pellet implanted mice, as compared with P pellet implanted, as presented in SF-4.

EPC Kinetics Through Human Menstrual Cycle

The morphology of cultured EPCs varied at different phases of the menstrual cycle (Figure 4A). At the preovulatory phase (T2), cultured EPCs, identified by double staining with acLDL-DiI and UEA-1-FITC, were recognized as isolated round adhesive cells, seldom forming colonies. After ovulation through the luteal phase (T3 to T5), EPCs appeared spindle-shaped, frequently exhibiting colony formation. Frequent colony formation was noted during the early proliferative phase (T1). The frequency of EPCs in culture decreased to the lowest level at the preovulatory phase (T2), increased gradually through ovulation, and remained high even during the early proliferative phase (Figure 4B).

As shown in Figure 4C, ovulation was identified between T2 and T3 by a surge of luteinizing hormone; the associated expression patterns of E2 and progesterone conform to the typical pattern of the menstrual cycle. VEGF levels were lowest at T1, then increased rapidly, reaching a peak at the T2 before slowly decreasing through the luteal phase. The pattern of VEGF expression was thus synchronized with E2. The numeric values of hormones and EPC numbers during menstrual cycle are shown in supplemental Table I.

Flow cytometrical analysis of PB-MNCs was used to determine the frequency of endothelial-specific antigen expressing cells as well as circulating immature EPCs according to the phase of the menstrual cycle. KDR was more frequently expressed by circulating cells from the preovulatory through luteal phases (Figure 4D-b). VE-cadherin antigen positive cells also increased, but the peak expression was until the later luteal phase. Differentiated ECs, positive for P1H12 antigen,[30] were identified at T1, immediately after menstruation, and did not augment, whereas KDR or VE-cadherin–positive endothelial lineage cells increased, after steroid hormone peaks (Figure 4D-b). Of note, the cell populations of CD133-positive or CD34-positive cells involving circulating immature EPCs in PB during the menstrual cycle disclosed a fluctuating pattern with significant amelioration at T3 following E2 peak (Figure 4D-c and 4D-d).

Discussion

The female reproductive system constitutes a unique exception to the quiescent vasculature of the normal healthy adult as the requirement for neovascularization recurring on a cyclic basis. Specifically, in every estrous cycle, the sequential maturation of the endometrium, as well as ovarian follicles and corpora lutea, is accompanied by concomitant development of elaborate capillary networks. Given the extent of newly forming vascular volume in endometrial

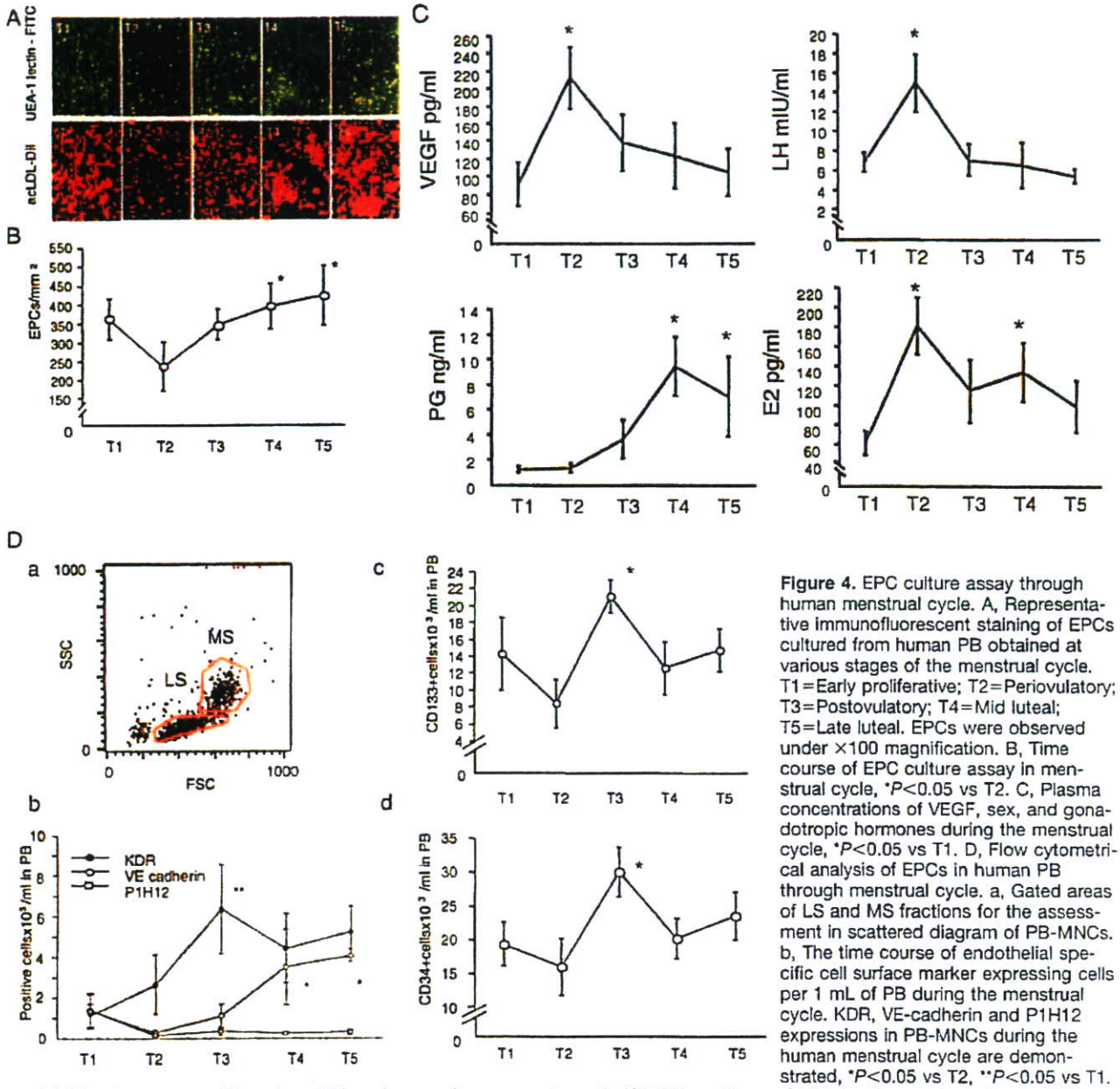

Figure 4. EPC culture assay through human menstrual cycle. A, Representative immunofluorescent staining of EPCs cultured from human PB obtained at various stages of the menstrual cycle. T1=Early proliferative; T2=Periovulatory; T3=Postovulatory; T4=Mid luteal; T5=Late luteal. EPCs were observed under ×100 magnification. B, Time course of EPC culture assay in menstrual cycle, *$P<0.05$ vs T2. C, Plasma concentrations of VEGF, sex, and gonadotropic hormones during the menstrual cycle, *$P<0.05$ vs T1. D, Flow cytometrical analysis of EPCs in human PB through menstrual cycle. a, Gated areas of LS and MS fractions for the assessment in scattered diagram of PB-MNCs. b, The time course of endothelial specific cell surface marker expressing cells per 1 mL of PB during the menstrual cycle. KDR, VE-cadherin and P1H12 expressions in PB-MNCs during the human menstrual cycle are demonstrated, *$P<0.05$ vs T2, **$P<0.05$ vs T1. c and d, The time course of immature EPC surface marker expressing cells (CD133-positive or CD34-positive cells) per 1 mL of PB, *$P<0.05$ vs T2.

development, it is possible that vasculogenic mechanisms may play a significant role in this cyclic organization. In this regard, we hypothesized that one of the main gender hormones, estrogen, controls EPC biology for cyclic neovascularization. The present findings provide evidence that the physiologic cycle of estrogen regulates EPC kinetics, ie, differentiation, proliferation, migration, apoptosis, mobilization, and ultimately incorporation into foci of neovascularization in the developing endometrium. Although the therapeutic potential of E2 for enhancing the contributions of EPCs for reendothelialization after vascular injury has been suggested, the physiological role of estrogen for EPC mediated vascular development has not been well established.[19,20,31]

Our EPC culture assay experiments demonstrated variations in EPC number and morphology throughout the phases of the menstrual cycle. These morphological changes are indicative of enhanced differentiation potential of circulating EPCs corresponding to cyclic hormonal changes. The peak increase in EPC number followed the peak serum concentrations of estrogen, as well as VEGF. This interval may potentially reflect a combination of estrogen effect on EPC proliferation, differentiation, and estrogen-induced mobilization from BM that has been suggested previously.[19,20,31]

The increase in the number of circulating EPCs expressing KDR or VE-cadherin antigen after peak estrogen levels and the decrease after downregulation of sex hormones were demonstrated by flow cytometrical analysis. Given their

essential function in embryonic vasculogenesis,[32-35] KDR and VE-cadherin were used to detect EPCs in PB-MNC population. Similarly, Strehlow et al have shown that estrogen mobilizes BM-derived EPCs (CD34 positive/KDR positive cells) into circulation of human subjects.[31] A temporal discrepancy in expression between KDR and VE-cadherin antigen in preovulatory and postovulatory phases was observed, which may suggest a differential effect of ovulatory estrogen on EPC biology. The basis for this differential expression may be related to the former findings that the expression of Flk-1 (homologue of mouse KDR) has been considered to represent a very early endothelial lineage marker during embryogenesis, whereas VE-cadherin–positive EPCs are considered differentiated from Flk-1–positive/VE-cadherin–negative cells.[35] The initial increase in KDR-positive cells seen during pre- to post-ovulatory phases may result from mobilization of immature EPCs into circulation, followed by an increase in committing EPCs during the luteal phase.[35] In contrast to KDR and VE-cadherin, P1H12 was used as a marker for differentiated ECs and was present at lesser frequency during preovulatory to luteal phases than other markers. Thus, differentiated ECs may circulate in PB only when dislodged by physiological blood vessel regression during menstruation.

The animal experiments provide potential insights into the significance of cyclic changes in EPC kinetics observed in human subjects. Systemic E2 pretreatment enhanced EPC mobilization detected in EPC culture assay and promoted enhanced neovascularization in the mouse cornea micropocket model. These results indicate that systemic estrogen stimulates EPC kinetics in the circulation, subsequently contributing to neovascularization via vasculogenesis. BMT experiments have demonstrated recruitment and incorporation of BM-derived Tie-2 receptor expressing cells, putative EPCs, during estrogen-induced endometrial development. It is intriguing to note that this pattern of EPC recruitment and incorporation is identical to the previously established pattern of in situ VEGF expression in the hormone-regulated cycle of endometrial development and regression.[3] In addition to EPCs found have incorporated into vascular structures, other round and at times even spindle-shaped cells were frequently identified in the uterine stroma. Regarding the finding, the cells could represent tissue macrophages derived from BM incorporating into uterine stroma during estrous cycle. The existence of BM-derived cells defined as macrophages (stained by F4/80) is also important to discuss because this may identify a significant role of blood bone cells in endometrial formation, especially regarding neovascularization. The similar findings were pointed out by several publications.[36,37] Tie-2 expressing BM-derived EPCs need vasculogenic environments introduced by angiogenic cytokines secreted from BM-derived macrophages. Therefore, this balance of EPCs and macrophages might play a pivotal role in neovascularization in endometrial formation.

Although the fate of the EPCs is currently uncertain, such cells may comprise EC reservoirs for the next round of endometrial development. The concept of BM-derived progenitor cell reservoirs in normal tissues is consistent with the notion of BM-derived satellite myoblasts and mesenchymal stem cells in muscle or other normal organs.[5,38] Using the same BMT models, we have previously demonstrated similar stroma-localized EPCs in growing neoplasms, wound healing, severe ischemia, and even though more sparsely—in normal organs.[17] Flk-1–positive cells previously demonstrated in the uterine myometrium[39] may represent similar cells. We have considered that the effect of estrogen may be direct or indirect (eg, mediated via VEGF). Evidence for a direct effect was given by the fact that EPC kinetics in CST male mice, lacking reproductive organs to respond to estrogen, responded equivalently in the case of OVX female mice, leaving a potentially estrogen-responsive (ie, VEGF-producing) uterus. This finding suggests that estrogen enhances EPC kinetics by direct interaction with EPCs or associated cells, such as in the BM microenvironment.

Our in vitro assay presented E2 promotion on EPC differentiation, migration, proliferation, and apoptosis inhibition, as partly indicated previously.[19,31] The findings that enhanced biological activities, such as proliferation, migration, antiapoptosis, and differentiation stimulated by E2 were blocked by an nonselective ERs antagonist (ICI), supported the fact that these effects of estrogen on EPCs were via functional ERs which were detected by mRNA in EPCs.

The importance of ERs on EPC bioactivity, using a myocardial infarcted model of ER α and ER β knockout mice has been recently documented by Hamada et al.[21] The authors described that ER α expressed in EPCs plays a more potent role in pathological vasculogenesis, rather than ER β. The present study disclosed the higher significance of ER α versus ER β in physiological vasculogenesis as well. During the culture period of human EPCs for 7 days through 4 days, the ER α expression was remained at the high level with the downregulation of ER β expression by real time PCR assay, as shown in Figure 1B. Accordingly, the EPC bioactivities disclosed in vitro study of day 7 cultured EPCs are considered to be brought through ER α. Furthermore, in vivo study of Tie-2/EGFP/BMT/OVX mice, the incorporated EPCs in uterus via E2 stimulation disclosed the expression of ER α, but not ER β, as shown in Figure 3E.

These findings may suggest that each ER shares the roles on EPC differentiation cascade, ie, the predominant function of ER β for EPC immature stage at provasculogenic state or ER α for EPC maturing stage at vasculogenic state, although the ER β function especially has yet to be elucidated.

Given the consideration, even in pathological vasculogenesis, ie, coronary vessel formation in infracted hearts, as shown by Hamada et al[21] as well as physiological vasculogenesis, each ER may have a unique role on EPC differentiation.

The basis for organogenesis has become a seminal issue for organ transplantation or therapeutic regeneration of damaged organs. Embryogenesis as well as physiological organogenesis in adult species reveal essential elements of organogenesis, devoid of pathological stimuli, including inflammation. The physiological regenerative processes constitute natural models that indicate how organs are established and survive. Blood vessel development is clearly one of the essential processes for organogenesis. The present study demonstrates that the unique system of cyclical blood vessel development and regression during the menstrual cycle, which occurs more

than 300 times in a female life span, involves hormone-mediated in situ proliferation, incorporation, differentiation, and survival of BM-derived progenitor cells. Above all, the unique EPC kinetics during menstrual cycle provides "dogma" for EPC biology as shown in supplemental Table I. Also, these findings have important implications for the impact of estrogen on vessel formation in disease states. Further insights regarding the precise mechanisms responsible for such physiological vasculogenesis will likely contribute to advanced methods and concepts for organ development in vivo as well as ex vivo.

Acknowledgments

This paper is dedicated to Dr. Jeffrey M. Isner. We would like to gratefully acknowledge him for his inspirational leadership, friendship and encouraging support. EPC colony assay was performed following the pretrial using cord blood under the approval of the ethical committees of Cord Blood Bank and Clinical Investigation in Tokai University School of Medicine. We also thank Dr. Kiyoshi Ando in Research Center for Regenerative Medicine for the management of the research facility; Dr. Yoshinori Okada and Dr. Jobu Itoh in Teaching and Research Support Center for the technical advices and supports; members of the animal facility in Tokai University School of Medicine as well as Miss. Sachie Ota as the secretary assistant. Especially, we greatfully thank Dr. Oren Tepper in Institute of Reconstructive Plastic Surgery, New York University Medical Center to finally check English grammar and style in the revised text.

Sources of Funding

This work was supported by grants from the National Institutes of Health (HL53354, and HL57516), Bethesda, MD; the ministry of Health, Labor and Welfare (H14-trans-001, H14-trans-002, H17-014), Japan; the ministry of Education, Culture, Sports, Science and Technology (Academic Frontier Promotion Program), Japan. H.M. is supported in part by Uehara Memorial Foundation and Kanagawa Nanbyo Foundation in Japan, and C.K. by a Cologne Fortune Grant in Germany. Estrogen receptor antagonist (ICI182,780) was kindly gifted by Astra Zeneca Pharmaceutical company.

Disclosures

None.

References

1. Reynolds LP, Killilea SD, Redmer DA. Angiogenesis in the female reproductive system. *FASEB J.* 1992;6:886–892.
2. Losordo DW, Isner JM. Estrogen and angiogenesis: A review. *Arterioscler Thromb Vasc Biol.* 2001;21:6–12.
3. Shweiki D, Itin A, Neufeld G, Gitay-Goren H, Keshet E. Patterns of expression of vascular endothelial growth factor (VEGF) and VEGF receptors in mice suggest a role in hormonally regulated angiogenesis. *J Clin Invest.* 1993;91:2235–2243.
4. Goede V, Schmidt T, Kimmina S, Kozian D, Augustin HG. Analysis of blood vessel maturation processes during cyclic ovarian angiogenesis. *Lab Invest.* 1998;78:1385–1394.
5. Ferrara N, Chen H, Davis-Smyth T, Gerber HP, Nguyen TN, Peers D, Chisholm V, Hillan KJ, Schwall RH. Vascular endothelial growth factor is essential for corpus luteum angiogenesis. *Nat Med.* 1998;4:336–340.
6. Spyridopoulos I, Sullivan AB, Kearney M, Isner JM, Losordo DW. Estrogen-receptor-mediated inhibition of human endothelial cell apoptosis. Estradiol as a survival factor. *Circulation.* 1997;95:1505–1514.
7. Gagliardi A, Collins DC. Inhibition of angiogenesis by antiestrogens. *Cancer Res.* 1993;53:533–535.
8. Morales DE, McGowan KA, Grant DS, Maheshwari S, Bhartiya D, Cid MC, Kleinman HK, Schnaper HW. Estrogen promotes angiogenic activity in human umbilical vein endothelial cells in vitro and in a murine model. *Circulation.* 1995;91:755–763.
9. Johns A, Freay AD, Fraser W, Korach KS, Rubanyi GM. Disruption of estrogen receptor gene prevents 17 beta estradiol-induced angiogenesis in transgenic mice. *Endocrinology.* 1996;137:4511–4513.
10. Lansink M, Koolwijk P, van Hinsbergh V, Kooistra T. Effect of steroid hormones and retinoids on the formation of capillary-like tubular structures of human microvascular endothelial cells in fibrin matrices is related to urokinase expression. *Blood.* 1998;92:927–938.
11. Gaunt SD, Pierce KR. Effects of estradiol on hematopoietic and marrow adherent cells of dogs. *Am J Vet Res.* 1986;47:906–909.
12. Medina KL, Kincade PW. Pregnancy-related steroids are potential negative regulators of B lymphopoiesis. *Proc Natl Acad Sci U S A.* 1994;91:5382–5386.
13. Erben RG, Raith S, Eberle J, Stangassinger M. Ovariectomy augments B lymphopoiesis and generation of monocyte-macrophage precursors in rat bone marrow. *Am J Physiol.* 1998;274:E476–E483.
14. Pacifici R, Brown C, Puscheck E, Friedrich E, Slatopolsky E, Maggio D, McCracken R, Avioli LV. Effect of surgical menopause and estrogen replacement on cytokine release from human blood mononuclear cells. *Proc Natl Acad Sci U S A.* 1991;88:5134–5138.
15. Folkman J, Klagsbrun M. Angiogenic factors. *Science.* 1987;235:442–447.
16. Asahara T, Murohara T, Sullivan A, Silver M, van der Zee R, Li T, Witzenbichler B, Schatteman G, Isner JM. Isolation of putative progenitor endothelial cells for angiogenesis. *Science.* 1997;275:964–967.
17. Asahara T, Masuda H, Takahashi T, Kalka C, Pastore C, Silver M, Kearne M, Magner M, Isner JM. Bone marrow origin of endothelial progenitor cells responsible for postnatal vasculogenesis in physiological and pathological neovascularization. *Circ Res.* 1999;85:221–228.
18. Takahashi T, Kalka C, Masuda H, Chen D, Silver M, Kearney M, Magner M, Isner JM, Asahara T. Ischemia- and cytokine-induced mobilization of bone marrow-derived endothelial progenitor cells for neovascularization. *Nat Med.* 1999;5:434–438.
19. Iwakura A, Luedemann C, Shastry S, Hanley A, Kearney M, Aikawa R, Isner JM, Asahara T, Losordo DW. Estrogen-mediated, endothelial nitric oxide synthase-dependent mobilization of bone marrow-derived endothelial progenitor cells contributes to reendothelialization after arterial injury. *Circulation.* 2003;108:3115–3121.
20. Iwakura A, Shastry S, Luedemann C, Hamada H, Kawamoto A, Kishore R, Zhu Y, Qin G, Silver M, Thorne T, Eaton L, Masuda H, Asahara T, Losordo DW. Estradiol enhances recovery after myocardial infarction by augmenting incorporation of bone marrow-derived endothelial progenitor cells into sites of ischemia-induced neovascularization via endothelial nitric oxide synthase-mediated activation of matrix metalloproteinase-9. *Circulation.* 2006;113:1605–1614.
21. Hamada H, Kim MK, Iwakura A, Ii M, Thorne T, Qin G, Asai J, Tsutsumi Y, Sekiguchi H, Silver M, Wecker A, Bord E, Zhu Y, Kishore R, Losordo DW. Estrogen receptors alpha and beta mediate contribution of bone marrow-derived endothelial progenitor cells to functional recovery after myocardial infarction. *Circulation.* 2006;114:2261–2270.
22. Asahara T, Takahashi T, Masuda H, Kalka C, Chen D, Iwaguro H, Inai Y, Silver M, Isner JM. VEGF contributes to postnatal neovascularization by mobilizing bone marrow-derived endothelial progenitor cells. *Embo J.* 1999;18:3964–3972.
23. Kalka C, Takahashi T, Masuda H, Asahara T, Isner JM. Vascular endothelial factor (VEGF): therapeutic angiogenesis and vasculogenesis in the treatment of cardiovascular disease. *Med Klin (Munich).* 1999;94:193–201.
24. Hubert JF, Vincent A, Labrie F. Estrogenic activity of phenol red in rat anterior pituitary cells in culture. *Biochem Biophys Res Commun.* 1986;141:885–891.
25. Berthois Y, Katzenellenbogen JA, Katzenellenbogen BS. Phenol red in tissue culture media is a weak estrogen: implications concerning the study of estrogen-responsive cells in culture. *Proc Natl Acad Sci U S A.* 1986;83:2496–2500.
26. Yamaguchi J, Kusano KF, Masuo O, Kawamoto A, Silver M, Murasawa S, Bosch-Marce M, Masuda H, Losordo DW, Isner JM, Asahara T. Stromal cell-derived factor-1 effects on ex vivo expanded endothelial progenitor cell recruitment for ischemic neovascularization. *Circulation.* 2003;107:1322–1328.
27. Asahara T, Chen D, Takahashi T, Fujikawa K, Kearney M, Magner M, Yancopoulos GD, Isner JM. Tie2 receptor ligands, angiopoietin-1 and angiopoietin-2, modulate VEGF-induced postnatal neovascularization. *Circ Res.* 1998;83:233–240.

28. Schlaeger TM, Qin Y, Fujiwara Y, Magram J, Sato TN. Vascular endothelial cell lineage-specific promoter in transgenic mice. *Development.* 1995;121:1089–1098.
29. Kalka C, Tehrani H, Laudenberg B, Vale PR, Isner JM, Asahara T, Symes JF. VEGF gene transfer mobilizes endothelial progenitor cells in patients with inoperable coronary disease. *Ann Thorac Surg.* 2000;70:829–834.
30. Solovey AA, Solovey AN, Harkness J, Hebbel RP. Modulation of endothelial cell activation in sickle cell disease: a pilot study. *Blood.* 2001; 97:1937–1941.
31. Strehlow K, Werner N, Berweiler J, Link A, Dirnagl U, Priller J, Laufs K, Ghaeni L, Milosevic M, Bohm M, Nickenig G. Estrogen increases bone marrow-derived endothelial progenitor cell production and diminishes neointima formation. *Circulation.* 2003;107:3059–3065.
32. Shalaby F, Rossant J, Yamaguchi TP, Gertsenstein M, Wu XF, Breitman ML, Schuh AC. Failure of blood-island formation and vasculogenesis in Flk-1-deficient mice. *Nature.* 1995;376:62–66.
33. Dumont DJ, Fong GH, Puri MC, Gradwohl G, Alitalo K, Breitman ML. Vascularization of the mouse embryo: a study of flk-1, tek, tie, and vascular endothelial growth factor expression during development. *Dev Dyn.* 1995;203:80–92.
34. Vittet D, Prandini MH, Berthier R, Schweitzer A, Martin-Sisteron H, Uzan G, Dejana E. Embryonic stem cells differentiate in vitro to endothelial cells through successive maturation steps. *Blood.* 1996;88:3424–3431.
35. Nishikawa SI, Nishikawa S, Hirashima M, Matsuyoshi N, Kodama H. Progressive lineage analysis by cell sorting and culture identifies FLK1+VE-cadherin+ cells at a diverging point of endothelial and hemopoietic lineages. *Development.* 1998;125:1747–1757.
36. Bonatz G, Hansmann ML, Buchholz F, Mettler L, Radzun HJ, Semm K. Macrophage- and lymphocyte-subtypes in the endometrium during different phases of the ovarian cycle. *Int J Gynaecol Obstet.* 1992;37:29–36.
37. Fernandez-Shaw S, Clarke MT, Hicks B, Naish CE, Barlow DH, Starkey PM. Bone marrow-derived cell populations in uterine and ectopic endometrium. *Hum Reprod.* 1995;10:2285–2289.
38. Pereira RF, Halford KW, O'Hara MD, Leeper DB, Sokolov BP, Pollard MD, Bagasra O, Prockop DJ. Cultured adherent cells from marrow can serve as long-lasting precursor cells for bone, cartilage, and lung in irradiated mice. *Proc Natl Acad Sci U S A.* 1995;92:4857–4861.
39. Brown LF, Detmar M, Tognazzi K, Abu-Jawdeh G, Iruela-Arispe ML. Uterine smooth muscle cells express functional receptors (flt-1 and KDR) for vascular permeability factor/vascular endothelial growth factor. *Lab Invest.* 1997;76:245–255.

Intramyocardial Transplantation of Autologous CD34$^+$ Stem Cells for Intractable Angina

A Phase I/IIa Double-Blind, Randomized Controlled Trial

Douglas W. Losordo, MD; Richard A. Schatz, MD; Christopher J. White, MD; James E. Udelson, MD; Vimal Veereshwarayya, PhD; Michelle Durgin, MHA; Kian Keong Poh, MD; Robert Weinstein, MD; Marianne Kearney, BS; Muqtada Chaudhry, MD; Aaron Burg, BS; Liz Eaton, BS; Lindsay Heyd, BS; Tina Thorne, BS; Leon Shturman, MD; Peter Hoffmeister, MD; Ken Story, PhD; Victor Zak, PhD; Douglas Dowling, BS; Jay H. Traverse, MD; Rachel E. Olson, MS; Janice Flanagan, RN; Donata Sodano, RN; Toshinori Murayama, MD; Atsuhiko Kawamoto, MD; Kengo Fukushima Kusano, MD; Jill Wollins, MD; Frederick Welt, MD; Pinak Shah, MD; Peter Soukas, MD; Takayuki Asahara, MD; Timothy D. Henry, MD

Background—A growing population of patients with coronary artery disease experiences angina that is not amenable to revascularization and is refractory to medical therapy. Preclinical studies have indicated that human CD34$^+$ stem cells induce neovascularization in ischemic myocardium, which enhances perfusion and function.

Methods and Results—Twenty-four patients (19 men and 5 women aged 48 to 84 years) with Canadian Cardiovascular Society class 3 or 4 angina who were undergoing optimal medical treatment and who were not candidates for mechanical revascularization were enrolled in a double-blind, randomized (3:1), placebo-controlled dose-escalating study. Patients received granulocyte colony-stimulating factor 5 $\mu g \cdot kg^{-1} \cdot d^{-1}$ for 5 days with leukapheresis on the fifth day. Selection of CD34$^+$ cells was performed with a Food and Drug Administration–approved device. Electromechanical mapping was performed to identify ischemic but viable regions of myocardium for injection of cells (versus saline). The total dose of cells was distributed in 10 intramyocardial, transendocardial injections. Patients were required to have an implantable cardioverter-defibrillator or to temporarily wear a LifeVest wearable defibrillator. No incidence was observed of myocardial infarction induced by mobilization or intramyocardial injection. The intramyocardial injection of cells or saline did not result in cardiac enzyme elevation, perforation, or pericardial effusion. No incidence of ventricular tachycardia or ventricular fibrillation occurred during the administration of granulocyte colony-stimulating factor or intramyocardial injections. One patient with a history of sudden cardiac death/ventricular tachycardia/ventricular fibrillation had catheter-induced ventricular tachycardia during mapping that required cardioversion. Serious adverse events were evenly distributed. Efficacy parameters including angina frequency, nitroglycerine usage, exercise time, and Canadian Cardiovascular Society class showed trends that favored CD34$^+$ cell–treated patients versus control subjects given placebo.

Conclusions—A randomized trial of intramyocardial injection of autologous CD34$^+$ cells in patients with intractable angina was completed that provides evidence for feasibility, safety, and bioactivity. A larger phase IIb study is currently under way to further evaluate this therapy. (***Circulation.*** **2007;115:3165-3172.)**

Key Words: angina ■ endothelium ■ stem cells ■ ischemia ■ angiogenesis

Despite the optimal use of antianginal medications and mechanical revascularization, a large number of patients with coronary artery disease remain severely symptomatic with disabling angina. It is estimated that 300 000 to 900 000 patients exist in the United States alone who have exhausted conventional medical therapies and continue to experience

Clinical Perspective p 3172

Received December 29, 2006; accepted April 11, 2007.

From Feinberg Cardiovascular Research Institute and Program in Cardiovascular Regenerative Medicine (D.W.L., V.V., M.D., T.T.), Division of Cardiovascular Medicine, Department of Medicine, Northwestern University Feinberg School of Medicine and Northwestern Memorial Hospital, Chicago, Ill; Division of Cardiovascular Medicine (D.W.L., V.V., M.D., K.K., R.W., M.K., M.C., A.B., L.E., L.H., T.T., L.S., P.H., V.Z., J.F., D.S., T.M., A.K., K.F.K., J.W., F.W., P. Shah, P. Soukas, T.A.), Department of Medicine, Caritas St. Elizabeth's Medical Center, Boston, Mass; Division of Cardiovascular Research (R.A.S.), Scripps Green Hospital, La Jolla, Calif; Department of Medicine (C.J.W.), Ochsner Clinic, New Orleans, La; Division of Cardiology (J.E.U.), Tufts-New England Medical Center, Boston, Mass; Baxter Healthcare (K.S.), Deerfield, Ill; Division of Cardiology (J.H.T., R.E.O., T.D.H.), Minneapolis Heart Institute, Minneapolis, Minn; and Cardiovascular Core Laboratories Inc (D.D.), Boston, Mass.

Clinical trial registration information—URL: http://www.clinicaltrials.gov. Unique identifier: NCT00081913.

Correspondence to Douglas W. Losordo, MD, Feinberg Cardiovascular Research Institute and Northwestern Memorial Hospital, Tarry 12-703, 303 E Chicago Ave, Chicago, IL 60611. E-mail d-losordo@northwestern.edu

Circulation is available at http://www.circulationaha.org DOI: 10.1161/CIRCULATIONAHA.106.687376